

DD^* potentials in chiral effective field theory and possible molecular states

Hao Xu^{1,2,3}, Bo Wang^{1,2,4,5}, Zhan-Wei Liu^{1,2,*} and Xiang Liu^{1,2,†}

¹*School of Physical Science and Technology, Lanzhou University, Lanzhou 730000, China*

²*Research Center for Hadron and CSR Physics, Lanzhou University & Institute of Modern Physics of CAS, Lanzhou 730000, China*

³*Department of Applied Physics, School of Science, Northwestern Polytechnical University, Xian 710129, China*

⁴*School of Physics and State Key Laboratory of Nuclear Physics and Technology, Peking University, Beijing 100871, China*

⁵*Center of High Energy Physics, Peking University, Beijing 100871, China*

The DD^* potentials are studied within the framework of heavy meson chiral effective field theory. We have obtained the effective potentials of the DD^* system up to $O(\epsilon^2)$ at one loop level. In addition to the one-pion exchange contribution, the contact and two-pion exchange interactions are also investigated in detail. Furthermore, we have searched for the possible molecular states by solving Schrödinger equation with the potentials. We notice that the contact and two-pion exchange potentials are non-negligible numerically and important for the existence of a bound state. In our results, no bound state is founded in the $I = 0$ channel within a wide range of cutoff parameter, while there exists a bound state in the $I = 1$ channel as cutoff is near m_ρ in our approach.

PACS numbers: 14.40.Pq, 13.25.Hw

I. INTRODUCTION

Chiral effective field theory (ChEFT) is an effective field theory respecting the chiral symmetry of Quantum chromodynamics (QCD) at low momenta. A prominent feature of ChEFT is that the results are expanded as a power series of small momenta rather than small coupling constants, which enables us to systematically study into the non-perturbative regime of the strong interaction. Pseudo-Goldstone bosons such as pion and kaon, with light masses, play very important roles for the low energy processes. Chiral symmetry constrains the form of the interaction quite strongly. Owing to the clear power counting scheme, ChEFT is very powerful to investigate the properties of light pseudoscalar bosons [1–3].

The situation becomes complicated when heavy hadrons involve. The power counting rule is broken because of large hadron masses. However, for the system with single heavy hadron and few light pseudoscalar bosons, the power counting scheme can be easily rebuilt, and many approaches of ChEFT have been developed to deal with the relevant scattering, interaction, electromagnetic moments, and other properties of such system. Heavy hadron chiral perturbation theory, the infrared regularization, and the extended-on-mass-shell scheme are frequently used in one heavy hadron sector [4–18]. Unfortunately, these approaches cannot be directly extended to study the properties about few heavy hadrons, like nuclear force.

Two-nucleon interaction bears another power counting problem. Two approximately on-shell nucleons in loop diagrams cause extra enhancement compared to the naive power counting, which prevents us from calculating scattering matrix directly. Weinberg proposed a framework to deal with the issue [19, 20]. One can first calculate an effective potential, i.e., sum of all two-particle irreducible (2PI) diagrams, and then iterate it with equations, such as Lippmann-Schwinger

and Schrödinger equation, to retrieve two-particle reducible (2PR) contributions. The Weinberg's formalism has been further extended and developed [21–24, 27, 29–35]. For example, a unitary transformation is presented to remove the energy dependence of the potential in Refs. [23, 24]. The renormalization of potentials are carefully studied in Refs. [25–29]. The authors in Ref. [30] revisit the nucleon-nucleon potential up to NNNLO within ChEFT. In Refs. [31, 32], the nucleon-antinucleon potential is investigated within ChEFT. Very recently, a covariant formalism of the N - N interaction is proposed in Ref. [33]. Three body and even four body nuclear forces have been systematically studied within ChEFT, see Refs. [34, 35] for a review. The application of ChEFT has been definitely advancing our understanding of the nuclear force [36].

With successes in the study of nuclear force, one may wonder whether ChEFT can help us to comprehend the interactions of heavy (charmed, bottomed) meson systems. Obviously, since heavy meson is heavier, we can make some assumptions such as the heavy quark limit without worries, and thus heavy hadron ChEFT is even more suitable than that in the nucleon system.

The XYZ and similar exotic states have attracted a lot of interest in the hadron physics, and it is well known the interaction between heavy mesons is quite responsible for the strange behavior at close threshold in charmonium and bottomonium spectra (see Ref. [37] for a review). This starts with the discovery of the famous $X(3872)$, which was observed by the Belle Collaboration in B decay process $B^{+-} \rightarrow K^{+-}\pi^+\pi^-J/\psi$ in 2003 [38]. $X(3872)$ is extremely close to the threshold of $D^0\bar{D}^{*0}$. Its mass is much smaller than quark model (such as the Godfrey-Isgur model [39]) predictions if it is regarded as $\chi'_{c1}(2P)$ charmonium, and moreover it has a large decay width for the isospin violation process $X(3872) \rightarrow J/\psi\rho$. After that, more and more XYZ and other exotic states candidates were discovered, such as recent observed pentaquark $P_c(4380)^+$ and $P_c(4450)^+$ [40] and still debated $X(5568)$ [41].

There are many models dealing with these states, such as the one-boson-exchange molecular model, some underlying multiquark models, kinematical effect, and so on (see the re-

*Electronic address: liuzhanwei@lzu.edu.cn

†Electronic address: xiangliu@lzu.edu.cn

view [37]). For example, in Refs. [42, 43] $D_{(s)}^* \bar{D}_{(s)}^*$ and DD^* systems are studied within the local hidden gauge formalism to dynamically generate $Y(3940)$, $Z(3930)$, $X(4160)$ and $Z_c(3900)$. In Ref. [44], the authors have investigated the DD^* system and its relation to $Z_c(3900)$ using the covariant spectator theory. $Z_c(3900)$ is also studied from the pole counting rule [45]. The authors in Ref. [46] have discussed $D^{(*)} \bar{D}^{(*)}$ with the constituent quark models, and solved the four-body Schrödinger equation with the Gaussian expansion method. The contact interaction of $DD^*(B\bar{B}^*)$ is specially investigated in Ref. [47] with the effective field theory, which is implemented with the heavy quark symmetry. The DD^* system is also intensively studied with different kinds of effective field theories, see Refs. [48–58] and many other works cited therein. For example, in Ref. [48], the authors studied the DD^* with XEFT using perturbative pions. In Ref [50], the authors studied $X(3872)$ and DD^* using non-perturbative pions. Moreover, the authors in Ref. [58] further included the effects of the D^* width. In Ref. [59], the study of hadronic molecules with effective field theories are reviewed.

As mentioned above, there are many models dealing with heavy meson systems. Among them, the one-boson-exchange model has interpreted many exotic phenomenas and made some predictions which have been verified by the later discoveries of new particles at experiment. This model can provide the dynamical potentials of hadron systems, and then one can solve the Schrödinger equation to see if there is a bound state. The model has been widely used to study the interaction of the two-heavy-hadron systems and related exotic states. The research of the charmed-anticharmed system and $X(3872)$ experiences a long progress. It starts from the pion and σ exchanges in early Ref. [60], directly extends to the multi-state exchanges [61], and then includes more complicated effects from S - D mixing [62], isospin violation [63], and so on. For the investigation of nuclear force, after the boson exchange model develops for decades (see the discussion in Ref. [64]), ChEFT is applied at last and help us systematically build the modern system of knowledge. Following their steps, it is natural to introduce ChEFT into the study of heavy meson systems after the one-boson-exchange model.

There exist many works on heavy mesons system with one-boson-exchange model and effective field theories, as mentioned above. It is interesting to investigate their higher order effects in chiral effective field theory, and then discuss the potential in coordinate space and search for the bound state by solving Schrödinger equation. We will also compare the results with one-boson-exchange model.

In this work, we focus on the doubly charmed-meson system DD^* , which is clearer than the hidden charmed system for the absence of annihilation channels. It provides us another insight to understand the heavy-flavor dynamics and non-perturbative QCD. Furthermore, it is analogous to deuteron since they both have contact, one-pion exchange (OPE), and two-pion exchange (TPE) contributions without annihilation channels in our framework.

Till now, the only observed doubly heavy-flavor system is the Ξ_{cc}^{++} baryon which was first discovered by SELEX collaboration [65]. Systems like ccu and ccd have been discussed

a lot, and their properties such as masses and electromagnetic moments still need more efforts to get clarified [69–76]. Very recently, LHCb group confirmed the existence of Ξ_{cc}^{++} but dis-favored the mass measured at SELEX [68]. With the technique and apparatus well developed nowadays, it is also possible to search for the doubly charmed boson made of DD^* at experiment.

In Ref. [77], the authors studied $D^{(*)} D^{(*)} (B^{(*)} B^{(*)})$ system to search for bound and resonant states, and they used pion and vector meson exchange potentials which are constrained by heavy quark symmetry and chiral symmetry. They found that in isospin 0 channel there exists a bound state in S -wave with binding energy 62.3 MeV, and no bound state is found in isospin 1 with S -wave. In Ref. [78] the authors have studied $D^{(*)} D^{(*)}$ system using the one-boson-exchange model, and found that there exists a bound state consisting of DD^* with binding energy 5 ~ 43 MeV in the isospin 0 channel. The authors in Ref. [79] investigate deuteron-like molecules with both open charm and bottom using the heavy-meson effective theory. In Ref. [80], charm-beauty meson bound states are dynamically generated from the $B^{(*)} D^{(*)}$ and $B^{(*)} \bar{D}^{(*)}$ interactions, and they also give the informations of the scattering lengths. There also exist lattice studies on BB and BB^* interaction [81–83]. Especially in Ref. [83], the authors considered both diquark-antidiquark and meson-meson configuration. In Ref. [84], we have investigated $\bar{B}\bar{B}$ interaction within heavy meson chiral effective field theory (HMChEFT). We obtain the potentials of the $\bar{B}\bar{B}$ system at one loop level, and have discussed the contact and two-pion exchange contributions in momentum space.

We investigate the DD^* system in this work. As we mentioned before, we need to study the potentials first, and then access physical observables indirectly. Furthermore, the potential in coordinate space can give us more intuitive information about interaction between mesons, and we can further solve a dynamic equation to see whether there exists a hadronic molecule. This paper is organized as follows. After introduction, we elucidate the framework in Sec. II. In Sec. III, we give results of potentials in momentum space. In Sec. IV, we study the potential in coordinate space to search possible molecules. At last, we summarize our conclusions.

II. LAGRANGIANS AND WEINBERG SCHEME

To study the DD^* system under HMChEFT, we need to show Lagrangians and provide results systematically in a strict power counting scheme. Our results are arranged order by order with the small parameter $\epsilon = p/\Lambda_\chi$, where p can be the momentum of pion, the residual momentum of heavy mesons, or the D - D^* mass splitting, and Λ_χ represents either the chiral breaking scale or the mass of the heavy mesons. In this work, flavor SU(2) symmetry is always kept.

A. Lagrangians at the leading order

At the leading order $O(\epsilon^0)$, both OPE diagrams and contact diagrams contribute to the amplitudes, and thus we should first build the Lagrangians for $DD^*\pi$ interaction vertices, the corresponding contact vertices, and so on.

The $DD^*\pi$ Lagrangian at leading order [85–87] is given by

$$\begin{aligned}\mathcal{L}_{H\phi}^{(1)} = & -\langle (iv \cdot \partial H) \bar{H} \rangle + \langle H v \cdot \Gamma \bar{H} \rangle + g \langle H \psi \gamma_5 \bar{H} \rangle \\ & - \frac{1}{8} \delta \langle H \sigma^{\mu\nu} \bar{H} \sigma_{\mu\nu} \rangle.\end{aligned}\quad (1)$$

In the above, H field represents the (D, D^*) doublet in the heavy quark limit

$$\begin{aligned}H &= \frac{1+\not{v}}{2} (P_\mu^* \gamma^\mu + iP \gamma_5), \\ \bar{H} &= \gamma^0 H^\dagger \gamma^0 = (P_\mu^{*\dagger} \gamma^\mu + iP^\dagger \gamma_5) \frac{1+\not{v}}{2}, \\ P &= (D^0, D^+), \quad P_\mu^* = (D^{*0}, D^{*+})_\mu.\end{aligned}\quad (2)$$

$v = (1, 0, 0, 0)$ stands for the 4-velocity of the H field. The last term in Eq.(1) is included to account for D - D^* mass shift which is not zero in the chiral limit, and δ is the mass difference in (D, D^*) doublet. The axial vector field u and chiral connection Γ are expressed as

$$\Gamma_\mu = \frac{i}{2} [\xi^\dagger, \partial_\mu \xi], \quad u_\mu = \frac{i}{2} \{\xi^\dagger, \partial_\mu \xi\}, \quad (3)$$

where $\xi = \exp(i\phi/2f)$, f is the bare constant for pion decay, and

$$\phi = \sqrt{2} \begin{pmatrix} \frac{\pi^0}{\sqrt{2}} & \pi^+ \\ \pi^- & -\frac{\pi^0}{\sqrt{2}} \end{pmatrix}. \quad (4)$$

The contact Lagrangian at $O(\epsilon^0)$ is constructed as follows [47, 51, 84]

$$\begin{aligned}\mathcal{L}_{4H}^{(0)} = & D_a \text{Tr}[H \gamma_\mu \bar{H}] \text{Tr}[H \gamma^\mu \bar{H}] \\ & + D_b \text{Tr}[H \gamma_\mu \gamma_5 \bar{H}] \text{Tr}[H \gamma^\mu \gamma_5 \bar{H}] \\ & + E_a \text{Tr}[H \gamma_\mu \tau^a \bar{H}] \text{Tr}[H \gamma^\mu \tau_a \bar{H}] \\ & + E_b \text{Tr}[H \gamma_\mu \gamma_5 \tau^a \bar{H}] \text{Tr}[H \gamma^\mu \gamma_5 \tau_a \bar{H}],\end{aligned}\quad (5)$$

where D_a, D_b, E_a, E_b are four independent low energy constants (LECs).

B. Lagrangians at the next to leading order

At chiral order $O(\epsilon^2)$, the total amplitudes consists of the contact corrections, OPE corrections, and TPE amplitudes. These one-loop amplitudes must be renormalized with the help of $O(\epsilon^2)$ Lagrangians. The divergences in the one-loop amplitudes are canceled by the infinite parts of the LECs in the following lagrangians [84],

$$\mathcal{L}_{4H}^{(2,h)} = D_a^h \text{Tr}[H \gamma_\mu \bar{H}] \text{Tr}[H \gamma^\mu \bar{H}] \text{Tr}(\chi_+)$$

$$\begin{aligned}& + D_b^h \text{Tr}[H \gamma_\mu \gamma_5 \bar{H}] \text{Tr}[H \gamma^\mu \gamma_5 \bar{H}] \text{Tr}(\chi_+) \\ & + E_a^h \text{Tr}[H \gamma_\mu \tau^a \bar{H}] \text{Tr}[H \gamma^\mu \tau_a \bar{H}] \text{Tr}(\chi_+) \\ & + E_b^h \text{Tr}[H \gamma_\mu \gamma_5 \tau^a \bar{H}] \text{Tr}[H \gamma^\mu \gamma_5 \tau_a \bar{H}] \text{Tr}(\chi_+),\end{aligned}\quad (6)$$

$$\begin{aligned}\mathcal{L}_{4H}^{(2,v)} = & \{D_{a1}^v \text{Tr}[(v \cdot DH) \gamma_\mu (v \cdot D \bar{H})] \text{Tr}[H \gamma^\mu \bar{H}] \\ & + D_{a2}^v \text{Tr}[(v \cdot DH) \gamma_\mu \bar{H}] \text{Tr}[(v \cdot DH) \gamma^\mu \bar{H}] \\ & + D_{a3}^v \text{Tr}[(v \cdot DH) \gamma_\mu \bar{H}] \text{Tr}[H \gamma^\mu (v \cdot D \bar{H})] + \\ & D_{a4}^v \text{Tr}[(v \cdot D)^2 H] \gamma_\mu \bar{H} \text{Tr}[H \gamma^\mu \bar{H}] \\ & + D_{b1}^v \text{Tr}[(v \cdot DH) \gamma_\mu \gamma_5 (v \cdot D \bar{H})] \text{Tr}[H \gamma^\mu \gamma_5 \bar{H}] + \dots \\ & + E_{a1}^v \text{Tr}[(v \cdot DH) \gamma_\mu \tau^a (v \cdot D \bar{H})] \text{Tr}[H \gamma^\mu \tau_a \bar{H}] + \dots \\ & + E_{b1}^v \text{Tr}[(v \cdot DH) \gamma_\mu \gamma_5 \tau^a (v \cdot D \bar{H})] \text{Tr}[H \gamma^\mu \gamma_5 \tau_a \bar{H}] \\ & + \dots\} + \text{H.c.},\end{aligned}\quad (7)$$

$$\begin{aligned}\mathcal{L}_{4H}^{(2,q)} = & \{D_1^q \text{Tr}[(D^\mu H) \gamma_\mu \gamma_5 (D^\nu \bar{H})] \text{Tr}[H \gamma_\nu \gamma_5 \bar{H}] \\ & + D_2^q \text{Tr}[(D^\mu H) \gamma_\mu \gamma_5 \bar{H}] \text{Tr}[(D^\nu H) \gamma_\nu \gamma_5 \bar{H}] \\ & + D_3^q \text{Tr}[(D^\mu H) \gamma_\mu \gamma_5 \bar{H}] \text{Tr}[H \gamma_\nu \gamma_5 (D^\nu \bar{H})] \\ & + D_4^q \text{Tr}[(D^\mu D^\nu H) \gamma_\mu \gamma_5 \bar{H}] \text{Tr}[H \gamma_\nu \gamma_5 \bar{H}] \\ & + E_1^q \text{Tr}[(D^\mu H) \gamma_\mu \gamma_5 \tau^a (D^\nu \bar{H})] \text{Tr}[H \gamma_\nu \gamma_5 \tau_a \bar{H}] \\ & + \dots\} + \text{H.c.}, \dots,\end{aligned}\quad (8)$$

where

$$\begin{aligned}\tilde{\chi}_\pm &= \chi_\pm - \frac{1}{2} \text{Tr}[\chi_\pm], \\ \chi_\pm &= \xi^\dagger \chi \xi^\dagger \pm \xi \chi \xi, \\ \chi &= m_\pi^2.\end{aligned}\quad (9)$$

Note that, the term $\mathcal{L}_{4H}^{(2,d)}$ in Ref. [84] vanishes in our SU(2) case.

In addition to canceling the divergences of the loop diagrams, the above Lagrangians also contain finite parts that contribute to tree-level diagrams at $O(\epsilon^2)$. They are governed by a large amount of LECs appearing in Eqs. (6)-(8).

C. Weinberg scheme

In this work, we adopt the power counting scheme from Weinberg to study the DD^* systems [19, 20]. This framework has been widely applied to nucleon-nucleon system as mentioned in the introduction. Let us start with a nucleon-nucleon TPE box diagram depicted in Fig. 1. As illustrated in Ref. [84], the amplitude can be written under the heavy hadron formalism:

$$\begin{aligned}& i \int d^4 l \frac{i}{l^0 + P^0 - \frac{\vec{q}_1^2}{2M_N} + i\epsilon} \frac{i}{-l^0 + P^0 - \frac{\vec{q}_2^2}{2M_N} + i\epsilon} \times \dots \\ & = i \int d^3 l \int dl^0 \frac{i}{l^0 + P^0 - \frac{\vec{q}_1^2}{2M_N} + i\epsilon} \frac{i}{-l^0 + P^0 - \frac{\vec{q}_2^2}{2M_N} + i\epsilon} \\ & \quad \times \dots \\ & = \int d^3 l \frac{\pi}{P^0 - \frac{1}{2} \left(\frac{\vec{q}_1^2}{2M_N} + \frac{\vec{q}_2^2}{2M_N} \right) + i\epsilon} \dots \\ & = \int d^3 l \frac{\pi}{\frac{\vec{P}^2}{(2M_N)} - \frac{1}{2} \left(\frac{\vec{q}_1^2}{2M_N} + \frac{\vec{q}_2^2}{2M_N} \right) + i\epsilon} \dots\end{aligned}$$

$$= - \int d^3l \frac{\pi}{\frac{\vec{p}}{(2M_N)} + i\epsilon} \dots, \quad (10)$$

where m_N is the mass of the nucleon, $\vec{q}_1 = \vec{P} + \vec{l}$ and $\vec{q}_2 = \vec{P} - \vec{l}$. Naive power counting gives the l^0 integral $O(|\vec{P}|^{-1})$, while we notice from Eq. (10) that the l^0 integral should be of $O(|\vec{P}|^{-2})$, i.e. the true order is enhanced by $|\vec{P}|^{-1}$. Such enhancement definitely violates the power counting rule, which would invalidate the chiral expansion. As pointed out in Ref. [19, 20], the origin of such a contradiction comes from double poles in Eq. (10) which relates to two-particle-reducible (2PR) part of the box diagram in Fig. 1.

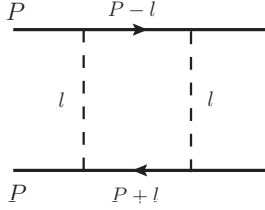


FIG. 1: A typical TPE box diagram of the nucleon-nucleon interaction. The solid line stands for the nucleon and the dashed line stands for the pion.

With the above analysis in mind, we just fall into the same situation when studying the interaction of the doubly-charmed meson pair, and thus can not directly calculate the scattering amplitude. Alternatively, we apply the Weinberg's power counting scheme. First, with the usual power counting rule, we compute the 2PI contributions of all diagrams, and this leads to effective potentials. Then we substitute the potentials into iterated equations such as Lippmann-Schwinger equation or Schrödinger equation to recover the 2PR contributions. Finally, we would obtain the desired scattering amplitudes or energy levels.

III. EFFECTIVE POTENTIALS OF DD^* SYSTEM

The effective potentials of DD^* system receive contributions from the contact and OPE diagrams at the leading order $O(\epsilon^0)$. At the next to leading order $O(\epsilon^2)$, there are both tree and one-loop corrections. The effective potentials \mathcal{V} are related to the Feynman amplitudes \mathcal{M} of 2PI diagrams

$$\mathcal{V} = \frac{-1}{4} \mathcal{M}, \quad (11)$$

which follows from the one-boson-exchange model despite some differences in conventions [90, 91].

At the lowest order $O(\epsilon^0)$, there are two diagrams at tree level illustrated in Fig. 2. They represent the contact and OPE contributions, individually. The contact terms mainly affect the short range interaction between particles while the OPE contribution determines the behavior of the long range interaction.

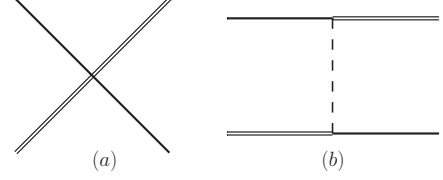


FIG. 2: Tree-level diagrams of the processes $DD^* \rightarrow DD^*$ at $O(\epsilon^0)$. The left diagram relates to the contact terms, and the right one is the one-pion-exchange diagram. The solid, double-solid, and dashed lines stand for D , D^* , pion, respectively.

With Lagrangians (1) and (5), the corresponding amplitudes can be easily computed. For the process $D(p_1)D^*(p_2) \rightarrow D(p_3)D^*(p_4)$ with isospin $I = 1$, the amplitudes for diagrams (a) and (b) in Fig. 2 read

$$\mathcal{M}_{I=1(a)}^{(0)} = i(-8D_a + 8D_b - 8E_a + 8E_b)\epsilon(p_2) \cdot \epsilon^*(p_4), \quad (12)$$

$$\mathcal{M}_{I=1(b)}^{(0)} = i(-1)\frac{g^2}{f^2} \frac{p_\mu p_\nu}{p^2 - m^2} \epsilon^\mu(p_2) \epsilon^{*\nu}(p_4). \quad (13)$$

For the process $D(p_1)D^*(p_2) \rightarrow D(p_3)D^*(p_4)$ with $I = 0$, the amplitudes are

$$\mathcal{M}_{I=0(a)}^{(0)} = i(24E_a + 24E_b - 8D_a - 8D_b)\epsilon(p_2) \cdot \epsilon^*(p_4), \quad (14)$$

$$\mathcal{M}_{I=0(b)}^{(0)} = i(-3)\frac{g^2}{f^2} \frac{p_\mu p_\nu}{p^2 - m^2} \epsilon^\mu(p_2) \epsilon^{*\nu}(p_4). \quad (15)$$

In above equations, momentum $p = p_1 - p_4$, the superscript (0) denotes the order $O(\epsilon^0)$, and the subscripts “ $I = 0, 1$ ” stand for the process $DD^* \rightarrow DD^*$ with isospin 0, 1, respectively.

At $O(\epsilon^2)$, a number of diagrams emerge. The tree diagrams at $O(\epsilon^2)$ are similar to Fig. 2 (a), but the vertices should be replaced with those from Lagrangians (6-8). There are additionally three sets of one-loop diagrams.

The diagrams in the first set are for one-loop corrections to the contact terms. They are depicted in Fig. 3. Diagrams (a12)-(a12) represents contributions from the wave function renormalization of external legs.

We show the second set of diagrams in Fig. 4. They represent one-loop corrections to the OPE diagrams. The diagrams (b1)-(b6) and (b8)-(b9) in Fig. 4 contribute to the renormalization of the $DD^*\pi$ vertex. Therefore, we must use the value for the bare coupling g in $\mathcal{M}^{(0)}$ at $O(\epsilon^0)$ to avoid double counting. We show the relation between the bare coupling g and the experiment coupling $g^{(2)}$ in Eq. (B1) in Appendix B. Similarly, the bare decay constant f should be used in Eqs. (13,15), too.

Final set is for the TPE diagrams which are illustrated in Fig. 5. They are important for the medium range interaction.

As discussed in the previous section, some diagrams, such as the box diagrams in Fig. 5, contain a 2PR part that should be subtracted. If there exists a loop function of a box diagram like

$$\int d^4l \frac{1}{v \cdot l + a + i\epsilon} \frac{1}{-v \cdot l - a + i\epsilon} \times \dots, \quad (16)$$

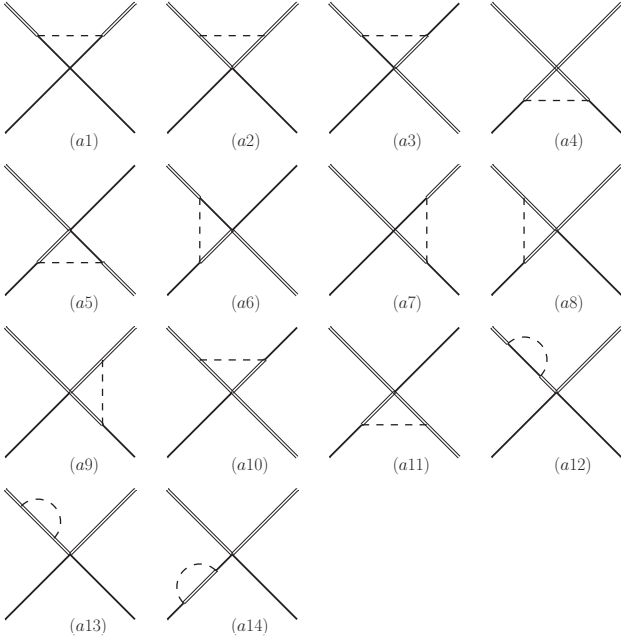


FIG. 3: One-loop corrections to the contact terms at $O(\epsilon^2)$. The solid, double-solid, and dashed lines stand for D , D^* , pion, respectively.

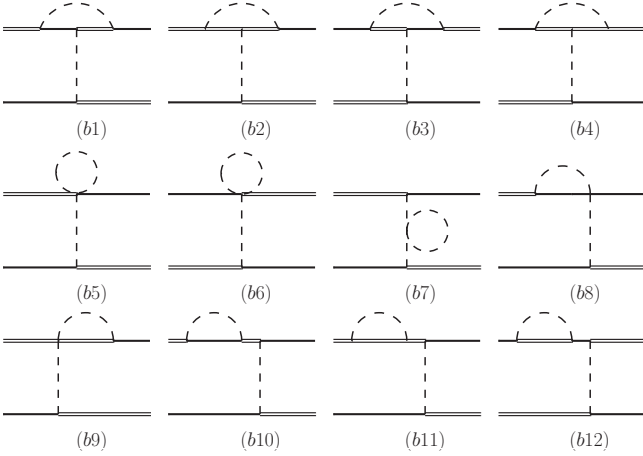


FIG. 4: One-loop corrections to the one-pion-exchange diagrams at $O(\epsilon^2)$. The solid, double-solid, and dashed lines stand for D , D^* , pion, respectively.

following Ref. [84, 88], we can separate the 2PR and 2PI parts by

$$\frac{1}{v \cdot l + a + i\epsilon} - \frac{1}{-v \cdot l - a + i\epsilon} = \frac{1}{v \cdot l + a + i\epsilon} \left[-\frac{1}{v \cdot l + a + i\epsilon} + 2\pi\delta(v \cdot l + a) \right]. \quad (17)$$

The term proportional to Dirac δ function is just the 2PR part which should be dropped in potentials.

All the one-loop amplitudes of the diagrams Figs. 3-5 for the processes $DD^* \rightarrow DD^*$ are shown in Appendix A. The

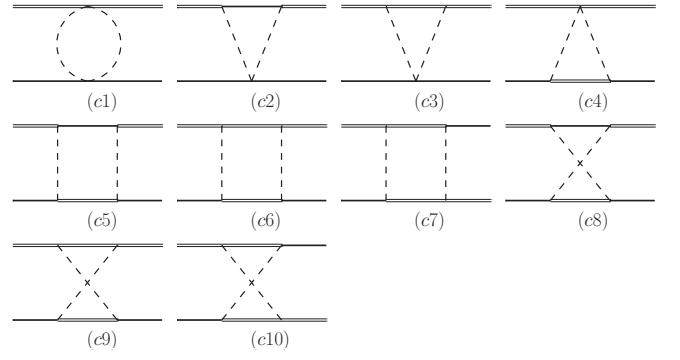


FIG. 5: Two-pion-exchange diagrams at $O(\epsilon^2)$. The solid, double-solid, and dashed lines stand for D , D^* , pion, respectively.

divergences of the loop functions are regularized with the dimensional regularization, and subtracted by the modified minimal subtraction scheme. Also, we list the definitions of the loop functions in Appendix C. The finite parts of the high order lagrangians should also contribute to tree level diagrams at $O(\epsilon^2)$, and they are governed by a large number of LECs. However, it needs plenty of data for DD^* (or other channels such as DD , DD) scattering in different partial waves to fit these LECs, but there is still lack now. Therefore in the present work, we only focus on the loop contributions at $O(\epsilon^2)$.

We can easily obtain the potentials $\mathcal{V}_{l=1}^{DD^*}$ and $\mathcal{V}_{l=0}^{DD^*}$ from the Feynman amplitudes by multiplying a factor $-1/4$. The polarized vectors in the potentials are delicately dealt with in Ref. [89]. In this work, we only consider the S -wave interaction, which leads to the following substitutions in Eqs. (12)-(15), (A1)-(A33)

$$\vec{\epsilon}(p_2) \cdot \vec{\epsilon}^*(p_4) \rightarrow 1, \quad (18)$$

$$\vec{\epsilon}(p_2) \cdot \vec{p} \vec{\epsilon}^*(p_4) \cdot \vec{p} \rightarrow \frac{1}{3} \vec{p}^2, \quad (19)$$

where we follow from the one-boson exchange model in Ref. [90, 91]. After all these procedures, the effective potentials $\mathcal{V}_{l=1}^{DD^*}$ and $\mathcal{V}_{l=0}^{DD^*}$ in the momentum space can be obtained. But, the potentials are energy dependent. A solution to this problem is proposed in Refs. [23, 24], where they apply a unitary transformation to get rid of the energy dependence. While in this work, we just take the transferred energies equal to zero, i.e. $p^0 = 0$ and $q^0 = 0$ for simplicity, as in the one-boson exchange model [60]. Also, we take the residual energies of the heavy mesons equal to zero, too.

IV. NUMERICAL RESULTS OF POTENTIALS IN MOMENTUM SPACE

We display input parameters for the numerical results: $m_\pi = 0.139$ GeV, the mass difference $\delta = 0.142$ GeV, $f_\pi = 0.086$ GeV, and renormalization scale $\mu = 4\pi f$. There are many works investigating the constant for $D^{(*)}D^{(*)}\pi$ coupling such as the lattice study [92–94], QCD sum rule [95–99], and other approaches [100–102]. The experimental process $D^* \rightarrow D\pi$

is fit to obtain the renormalized coupling $g^{(2)}$ [103], and we get the bare coupling $g = 0.65$ by using the $O(\epsilon^2)$ correction in Eq. (B1).

First, we list the results for the contact contributions. For $\mathcal{V}_{I=1}^{DD^*}$ in the channel of isospin 1, the effective potential at $O(\epsilon^0)$ and $O(\epsilon^2)$ is as follows

$$\mathcal{V}_{I=1}^{(0)} = -2D_a + 2D_b - 2E_a + 2E_b, \quad (20)$$

$$\mathcal{V}_{I=1}^{(2)} = -(0.253 + 0.031i)D_b + 0.044E_a - (0.166 + 0.030i)E_b. \quad (21)$$

And for the channel of isospin 0, we obtain

$$\mathcal{V}_{I=0}^{(0)} = -2D_a - 2D_b + 6E_a + 6E_b, \quad (22)$$

$$\mathcal{V}_{I=0}^{(2)} = -(1.214 + 0.190i)E_a + (0.116 + 0.047i)D_b + (0.025 - 0.143i)E_b. \quad (23)$$

Obviously, the contact contributions are just constants, and they result in $\delta(r)$ potentials in coordinate space, which describes short distance effect. From Eqs. (20)-(23), we see the convergence of the series expansion is good. From Eqs. (21) and (23), the contact coupling constant D_a does not appear in the effective potential at $O(\epsilon^2)$ because the contributions from D_a term are canceled among various diagrams in Fig. 3.

Next, we focus on the properties of the OPE and TPE contributions. We illustrate the corresponding potentials for channels with isospin 0 and 1 in Figs. 6 and 7, respectively, ranging from $q = |\mathbf{q}| = 0$ to 300 MeV.

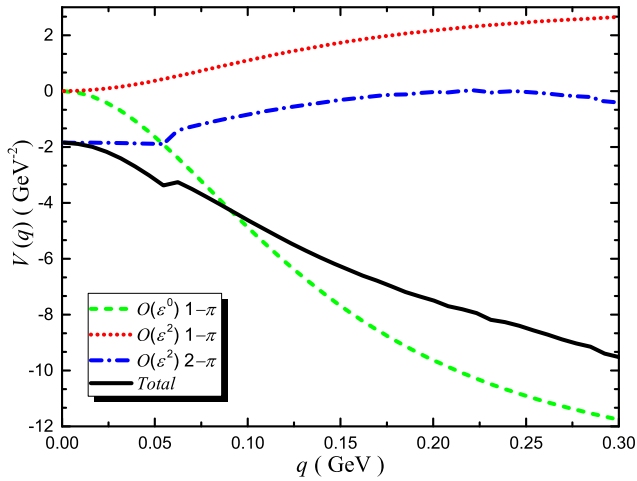


FIG. 6: (color online). OPE and TPE potentials $\mathcal{V}_{I=0}^{DD^*}$ for isospin-0 channel. q stands for the three momentum in unit of GeV, y axis represents the effective potential in unit of GeV^{-2} . The red dotted and green dashed lines describe the OPE potentials at the leading and next to leading order, individually. The blue dot-dashed line is for the TPE potential. The sum of the three contributions is represented by the black solid line.

From Figs. 6 and 7, one can see that the OPE contributions at $O(\epsilon^0)$ are dominant in both the $I = 0$ and $I = 1$ channels since the green dashed lines are close to the black solid ones. The OPE potentials at $O(\epsilon^2)$ are small comparing to

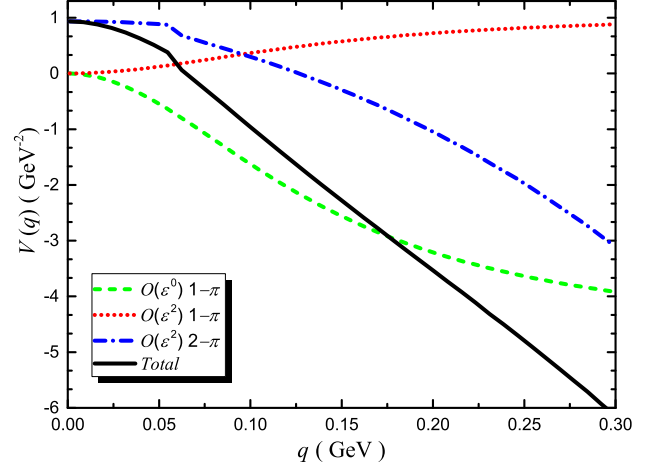


FIG. 7: (color online). OPE and TPE of the potentials $\mathcal{V}_{I=1}^{DD^*}$. The line types and color schemes match those of Fig. 6.

those at $O(\epsilon^0)$. The sums of OPE contributions are negative from Figs. 6 and 7, which means the OPE interaction is attractive in both the $I = 0$ and $I = 1$ channels. We also notice that the OPE interaction in $I = 0$ is more attractive than $I = 1$.

The situation for the TPE potentials is more complicated. The TPE contributions behave differently in $I = 0$ and $I = 1$ channels. In Fig. 6, the TPE interaction for $I = 0$ channel is attractive in the range $0 \sim 300$ MeV, and it tends to grow beyond 300 MeV. The TPE potential at $O(\epsilon^2)$ is larger than the OPE one at $O(\epsilon^0)$ in the range $0 \sim 60$ MeV, while the OPE contribution exceeds that of TPE rapidly when q is larger than 60 MeV, and becomes dominant. We can say that the convergence of the chiral series is good. Looking at Fig. 7, we see the TPE potential is repulsive in the range $0 \sim 120$ MeV, while it becomes attractive as q is beyond the range. The TPE potential at $O(\epsilon^2)$ is smaller than the OPE contribution at $O(\epsilon^0)$ in the lower range of the momentum, and becomes comparable in large momenta. It seems to indicate the convergence of the chiral series would be spoiled at larger transferred momenta. From the blue dot-dashed lines in Figs. 6 and 7, we see the TPE interaction in $I = 1$ is more attractive than that in $I = 0$.

Let us turn to the sum of these three contributions. The total contribution in Fig. 6 for $\mathcal{V}_{I=0}^{DD^*}$ is attractive, while in Fig. 7 for $\mathcal{V}_{I=1}^{DD^*}$ it is less attractive and tends to repulsive as q becomes smaller than 50 MeV because of the repulsive TPE contribution. It makes us wonder whether there could form a bound state in the DD^* system with the inclusion of contact contributions.

V. POTENTIALS IN COORDINATE SPACE AND POSSIBLE MOLECULAR STATE

Although the pion exchange interaction is attractive at most momenta, there can still be no bound states if not attractive enough. Moreover, the contact interaction might be repulsive and furthermore decrease the possibility for the existence of

a bound state. Thus the contact potentials must be first obtained numerically by the determination of the LECs. After that, we can investigate the effective potentials in coordinate space, and then solve the Schrödinger equation to search for possible molecular states.

A. Determination of LECs

We determine the LECs in the contact contributions (20)-(23) with the resonance saturation model [64, 104–107]. We assume these short-range couplings result from the ρ and ϕ exchanges as in Ref. [108], as well as other meson exchanges (scalar and axial-vector). Although it may be a rough estimate, it is meaningful to make such an attempt. The $D^{(*)}D^{(*)}V$ Lagrangian respecting heavy quark symmetry and U(2) flavor symmetry is given by [78]

$$\mathcal{L}_{HHV} = i\beta\langle H\gamma_\mu(V^\mu - \rho^\mu)\bar{H}\rangle + i\lambda\langle H\sigma_{\mu\nu}F^{\mu\nu}(\rho)\bar{H}\rangle. \quad (24)$$

In the above, H is the same as Eq. (2), $F_{\mu\nu} = \partial_\mu\rho_\nu - \partial_\nu\rho_\mu - [\rho_\mu, \rho_\nu]$ with $\rho_\mu = \frac{ig_v}{\sqrt{2}}\hat{\rho}_\mu$, and the multiplet $\hat{\rho}$ is defined by

$$\hat{\rho}^\mu = \begin{pmatrix} \frac{\rho^0}{\sqrt{2}} + \frac{\omega}{\sqrt{2}} & \rho^+ \\ \rho^- & -\frac{\rho^0}{\sqrt{2}} + \frac{\omega}{\sqrt{2}} \end{pmatrix}^\mu. \quad (25)$$

The coupling constants $g_v = 5.8$, $\lambda = 0.56 \text{ GeV}^{-1}$ and $\beta = 0.9$ [78]. As for the scalar exchanges S (σ , f_0 , a_0), we use [78, 107]:

$$\mathcal{L}_{HHS} = g_{HHS}\langle H S \bar{H}\rangle, \quad (26)$$

where $g_{HHa_0(f_0)} = \sqrt{3}g_{HH\sigma}$ [107], $g_{HH\sigma} = \frac{g_\pi}{2\sqrt{6}}$ and $g_\pi = 3.73$ [115]. For the axial-vector mesons A_V (a_1 , f_1), we use

$$\mathcal{L}_{HHA_V} = g_{HHA_V}\langle H\gamma_\mu\gamma_5 A_V^\mu\bar{H}\rangle. \quad (27)$$

After matching the meson exchange amplitudes to the contact amplitudes with 4 independent isospin channels of $D^{(*)}D^{(*)} \rightarrow D^{(*)}D^{(*)}$, we obtain

$$D_a = -\frac{\beta^2 g_v^2}{8m_\omega^2} - \frac{g_s^2}{2m_\sigma^2} - \frac{g_{s0}^2}{12m_{f_0}^2}, \quad E_a = -\frac{\beta^2 g_v^2}{8m_\rho^2} - \frac{g_{s0}^2}{4m_{a_0}^2},$$

$$D_b = \frac{g_{HHA_V}^2}{8m_{a_1}^2}, \quad E_b = \frac{g_{HHA_V}^2}{8m_{f_1}^2}. \quad (28)$$

However, we can not find any inputs for axial-vector meson coupling g_{HHA_V} , and therefore we simply assume the low-energy constants are saturated by resonances with masses below 800 MeV. We estimate their errors with the contributions from the other four particles, f_0 , a_0 , f_1 , and a_1 . $|g_{HHA_V}|$ is roughly set to $\beta g_v \sim 5$. We finally get the numerical values:

$$D_a = -6.62 \pm 0.15, \quad E_a = -5.74 \pm 0.45,$$

$$D_b = 0 \pm 1.96, \quad E_b = 0 \pm 1.89. \quad (29)$$

B. Potentials in coordinate space

After the determination of the LECs, we are ready to transfer the potentials into coordinate space:

$$\mathcal{V}(\mathbf{r}) = \int \frac{d\mathbf{q}}{(2\pi)^3} \mathcal{V}(\mathbf{q}) e^{i\mathbf{q}\cdot\mathbf{r}}. \quad (30)$$

However, since $\mathcal{V}(\mathbf{q})$ in ChEFT is proportional to the power series of \mathbf{q} , the higher order terms diverge worse. The evaluation of $\mathcal{V}(\mathbf{r})$ is essentially a non-perturbative problem, and it originates from the resummation of the 2PI potentials. We have to regularize Eq. (30) non-perturbatively. Enormous efforts have been made to explore the non-perturbative renormalization, such as Refs. [21, 23, 109–114]. Here we resort to a simple Gaussian cutoff $\exp(-\vec{p}^{2n}/\Lambda^{2n})$ to suppress the higher momentum contributions, as in Ref. [22, 24, 33]. We use $n = 2$ as in Ref. [33]. In the nucleon-nucleon ChEFT, the value of cutoff parameter is commonly below the ρ meson mass [30], and therefore we adopt $\Lambda = 0.7 \text{ GeV}$ in our work.

The resulting full potentials are shown in Figs. 8 and 9, where we set $\Lambda = 0.7 \text{ GeV}$. From Figs. 8 and 9, we find the OPE and TPE interactions are attractive in both cases, and the contact terms lead to the attractive interaction in the $I = 0$ channel while repulsive interaction in the $I = 1$ channel. Obviously, this difference brings more opportunity to form a bound state in the $I = 0$ channel than in the $I = 1$ channel. Let us focus on the total results. The total potential in the short distance for the $I = 1$ channel is repulsive but small while that for the $I = 0$ channel is attractive and large.

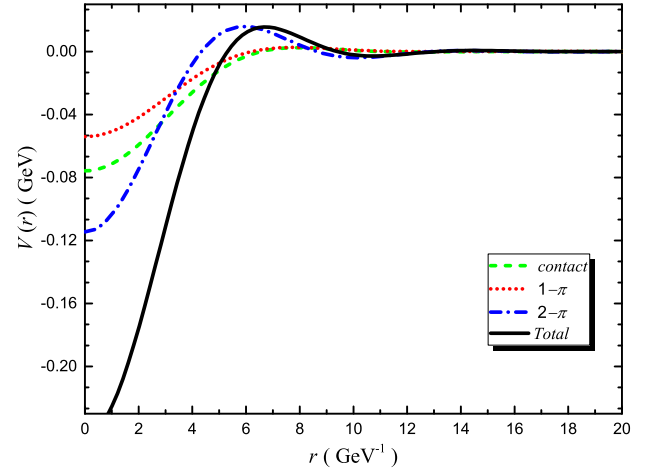


FIG. 8: (color online). S -wave potentials of the DD^* system with $I = 0$ in units of GeV. The green dashed, red dotted, and blue dot-dashed lines stand for the contact, OPE, and TPE contributions, respectively. The full potential is drawn in black solid line.

C. Possible bound states

With the potentials in hand, we are finally able to solve Schrödinger equation. We find a bound state with the bind-

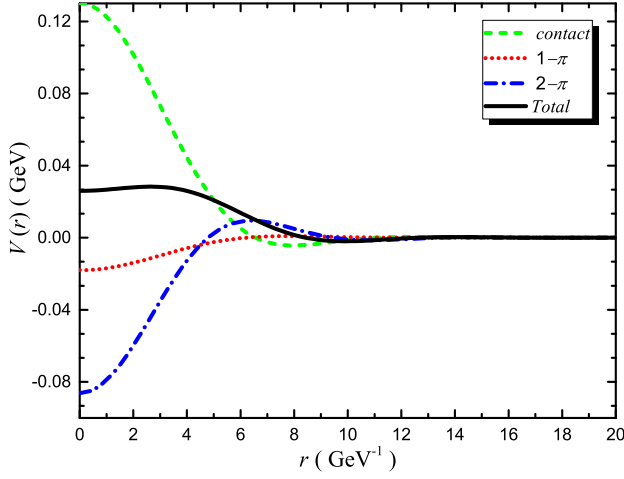


FIG. 9: (color online). S -wave potentials of the DD^* system with $I = 1$ in units of GeV. The line types and color schemes match those of Fig. 8.

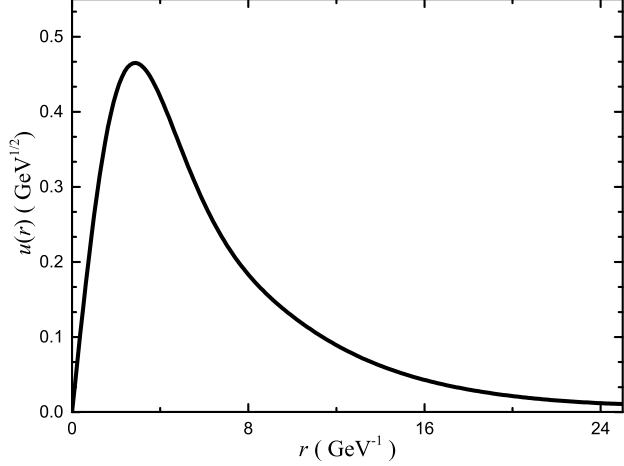


FIG. 10: (color online). The radial wave function with the full potential depicted in Fig. 8.

ing energy around 17.5 MeV in the $I = 0$ channel, and there exists no bound state in the $I = 1$ channel.

The radial wave function for the $I = 0$ channel is plotted in Fig. 10. It extends to quite large distance, which means the constituents D and D^* are separated.

It is worthwhile noticing that in pion and vector meson exchange potential model [77], they found a bound state with binding energy 62.3 MeV in $I = 1$ channel while no state is found in $I = 1$ channel. In the one-boson exchange model, there is also a bound state in the $I = 0$ channel, and the binding energy is about 5 ~ 43 MeV with a reasonable cutoff [78]. No bound state was found in the $I = 1$ channel in that model, either [78]. Our results are consistent.

From Fig. 9, we notice the contact interaction is repulsive at short distance. However, we cannot still find a bound state even if dropping the contact interaction in the $I = 1$ chan-

nel, which states the pion exchange interaction is not attractive enough for binding DD^* . If we repeat and turn off the contact potential in the $I = 0$ channel, the shallow bound state will disappear. We cannot obtain a reasonable energy eigenvalue of the Schrödinger equations, either, if keeping the OPE potentials themselves for two channels. The attractive contact and TPE interactions are important for the existence of the molecule in the $I = 0$ channel.

Theoretically, the obtained observable (such as binding energy) is independent of the regularization procedure in Eq. (30). The formal dependence on the cutoff Λ in Eq. (30) can be compensated by the Λ dependence of the LECs. However, the results are sometimes sensitive with different choices of Λ in practice. Here we investigate the influence of the cutoff with the LECs fixed. We plot the full potentials with different cutoffs in Fig. 11. From the figure, we notice that the potential becomes deeper and steeper in the short range as the cutoff increases. After solving Schrödinger equation, we obtain the binding energy 1.1 MeV, 17.5 MeV and 53.1 MeV with $\Lambda = 0.6, 0.7$ GeV, and m_ρ , respectively. The binding energy is sensitive to the cutoff. However, bound state solution exists as cutoff is near m_ρ . Furthermore, as we stressed earlier, the cutoff dependence can be compensated if readjusting the LECs at different cutoffs.

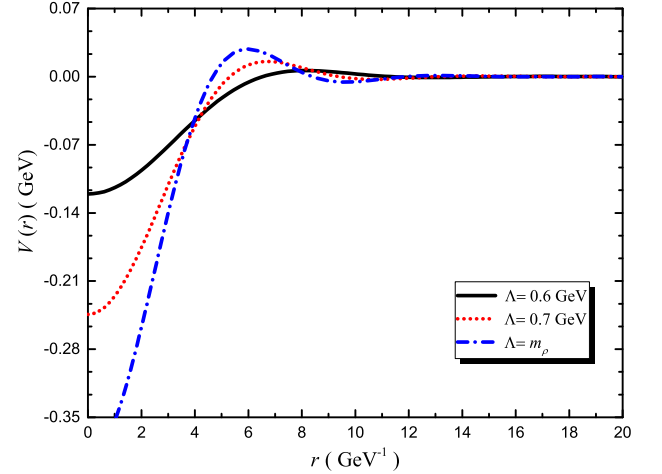


FIG. 11: (color online). The total potentials of the DD^* system in the S wave with $I = 0$, where three cutoff values are adopted.

There also exist other sources of uncertainties. Firstly, we discuss the uncertainty from the resonance saturation model which is utilized to determine LECs of contact terms. From the numerical values of D_a and E_a in Eq. 29, we can see the contributions from f_0 and a_0 are small, and ρ , ω and σ exchanges dominate D_a and E_a . For D_b and E_b in Eq. 29, the uncertainty brought by axial-vector exchanges are not small, and therefore they have considerable effects on binding energy. However the estimation of the axial-vector contributions is quite rough, we hope we can obtain much more reliable input for g_{HHV_A} in the future. In general, the uncertainty in Eq (29) gives the binding energy at $\Lambda = 0.7$ GeV: $17.5^{+4.1+18.3}_{-3.9-14.0}$ MeV, where the first uncertainty comes from f_0 and a_0 , and

the second uncertainty comes from axial-vector mesons (a_1 , f_1).

Secondly, the uncertainty can come from that of axial coupling g . When we include the experimental error [103] (width and branching fraction), we obtain the bare coupling $g = 0.65^{+0.02}_{-0.01}$, and the binding energy in $I = 0$ channel with $\Lambda = 0.7$ GeV is $17.5^{+9.6}_{-3.9}$ MeV. We can see the binding energy is sensitive to the coupling g , but not much sensitive as cutoff Λ . Including the uncertainty of $D_{a(b)}$, $E_{a(b)}$ discussed above, we obtain the binding energy $17.5^{+21.1}_{-15.0}$ at $\Lambda = 0.7$ GeV. This uncertainty is largely brought by axial-vector mesons, the uncertainty from g is moderate, and the uncertainty from f_0 and a_0 is smallest.

The third uncertainty comes from truncation error. Here we partially estimate few loop diagrams of contact contribution at $O(\epsilon^4)$ to show how large the truncation error is. For $O(\epsilon^4)$ contact loop contribution, there exist many Feynmann diagrams. We pick some diagrams and plot them in Fig. 12. In the first four diagrams of Fig. 12, each one contains two

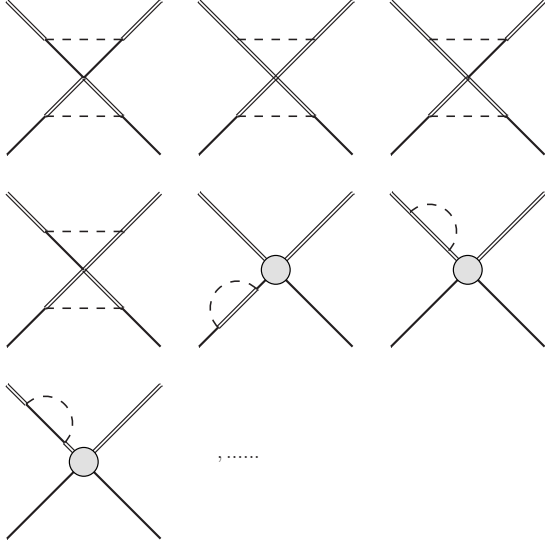


FIG. 12: Some loop diagrams related to contact terms at $O(\epsilon^4)$. The last three diagrams indicate the contribution from wavefunction renormalization to the contact loop diagrams at $O(\epsilon^2)$ in Fig. 3.

separated loops, and the sum of these reads:

$$\begin{aligned} \mathcal{V}_{I=1}^{(4)} &\sim (-0.00016 - 0.00015i)(D_a - D_b + E_a - E_b), \\ \mathcal{V}_{I=0}^{(4)} &\sim (-0.0039 - 0.0014i)D_a + (0.0117 + 0.0041i)E_a \\ &\quad + (0.0043 + 0.0019i)D_b - (0.0129 + 0.0057i)E_b. \end{aligned} \quad (31)$$

We can see they are generally $O(\frac{1}{100})$ relative to those at $O(\epsilon^2)$ by comparing with Eqs. (21) and (23). The last three set of diagrams in Fig. 12 indicate the wave function renormalization of the $O(\epsilon^2)$ diagrams in Fig. 3, and the sum of these reads:

$$\begin{aligned} \mathcal{V}_{I=1}^{(4)} &\sim (0.0196 + 0.0060i)D_b - 0.0034E_a \\ &\quad + (0.0127 + 0.0047i)E_b, \end{aligned} \quad (32)$$

$$\begin{aligned} \mathcal{V}_{I=0}^{(4)} &\sim (0.0934 + 0.0321i)E_a - (0.0085 + 0.0054i)D_b \\ &\quad - (0.0039 - 0.0110i)E_b. \end{aligned} \quad (33)$$

They are $O(\frac{1}{10})$ relative to those at $O(\epsilon^2)$ from Eqs. (21) and (23). Therefore we expect when all the contact $O(\epsilon^4)$ diagrams are included, the convergence may not be bad.

VI. SUMMARY

In this work, we have systematically studied the DD^* system with ChEFT. Due to the intrinsic difficulty of the ChEFT, we cannot obtain the physical observables directly from the Feynman diagrams. We alternatively calculate the potentials, i.e., the sum of all the 2PI diagrams, and then iterate them into Lippmann-Schwinger or Schrödinger equation to recover the 2PR contributions.

We have investigated the DD^* effective potentials in ChEFT with Weinberg scheme. With the effective potentials obtained in momentum space, we have analyzed the contact, OPE and TPE contribution in detail. The OPE and TPE contributions are free of many LECs, and thus they are more model independent than the contact interaction since the LECs are determined with the resonance saturation model in this work. The OPE contribution at $O(\epsilon^2)$ is smaller than that at $O(\epsilon^0)$. The potential from TPE at $O(\epsilon^2)$ is relatively large compared to that from OPE at $O(\epsilon^0)$ in the $I = 1$ channel, while it shows a good convergence in the $I = 0$ channel. The TPE interaction is important and non-negligible.

We have determined the LECs in contact contributions with the resonance saturation model, and further explored the full potentials in coordinate space, which are regularized with a simple Gaussian cutoff. The roles of each contributions have been discussed, and the total potentials are very different in two channels. We have also discussed the importance of the contact contribution and the influence of the cutoff in detail. Furthermore, we discuss the uncertainties of our approach, which comes from axial coupling g , LECs and truncation error. We find that the TPE contribution is non-negligible and attractive in general, while the contact contributions is an important element to compete the π -exchange contributions and cause quite different behavior in each channels. Despite the roughly estimated LECs, we notice that no bound state exists in the $I = 1$ channel in a wide range of cutoff parameter, while there exists a bound state in the $I = 1$ channel as cutoff is near m_ρ in our approach. The binding energy is sensitive to the cutoff. Our results are consistent with those in the one-boson-exchange model [78].

In this work, we have ignored many other sub-leading effects from the isospin violation, S - D mixing, recoiling, and so on. These effects can be investigated in future, and our framework shall be proved to be elegant.

We point out that the DD^* molecule may be discovered at experiments through various processes. Since at Tevatron and LHCb there are a number of B_c events, the DD^* molecule can be produced via B_c weak decay: singly Cabibbo-suppressed process $B_c \rightarrow X(DD^*)K$, doubly Cabibbo-suppressed processes $B_c \rightarrow X(DD^*)\pi$ and $B_c \rightarrow X(DD^*)D$. Moreover we

hope the e^+e^- process such as $e^+e^- \rightarrow X(DD^*)\bar{D}\bar{D}$ at BelleII can be studied to observe the state. The molecular states may be constructed through DD final states. We also expect the lattice simulations to test our results.

Our exploration of the DD^* system can help to make more profound understanding of the heavy meson system and non-perturbative QCD. We expect our results can be tested by future LHCb and BelleII experiments, and help the extrapolations of future lattice simulations.

Acknowledgments

We would like to thank Professor Shi-Lin Zhu for useful suggestion. Xu also thanks Rui Chen and Ming-Xiao Duan for helpful discussions. This project is supported by the National Natural Science Foundation of China under Grants No. 11705072. This work is also supported by the Fundamental Research Funds for the Central Universities. Xiang Liu is also supported by the China National Funds for Distinguished Young Scientists under Grants No. 11825503.

Appendix A: One-loop amplitudes of the processes $DD^* \rightarrow DD^*$ at $O(\epsilon^2)$

We first list the amplitudes of the process $D(p_1)D^*(p_2) \rightarrow D(p_3)D^*(p_4)$. The difference between the amplitudes for the $I = 0$ and $I = 1$ channels is just a factor.

For the one-loop corrections to the contact terms in Fig. 3, the Feynman amplitudes are

$$\mathcal{M}_{(a1)}^{(2)} = \frac{-i g^2}{4 f^2} A_{a1} J_{22}^g(m, \omega_1, \omega_2) \varepsilon(p_2) \cdot \varepsilon^*(p_4) \quad (\text{A1})$$

with $\omega_1 = v \cdot p_2 - M$, $\omega_2 = v \cdot p_4 - M$;

$$\mathcal{M}_{(a2)}^{(2)} = \frac{-i g^2}{2 f^2} A_{a2} J_{22}^g(m, \omega_1, \omega_2) \varepsilon(p_2) \cdot \varepsilon^*(p_4) \quad (\text{A2})$$

with $\omega_1 = v \cdot p_2 - M - \delta$, $\omega_2 = v \cdot p_4 - M - \delta$;

$$\mathcal{M}_{(a3)}^{(2)} = \frac{i g^2}{4 f^2} A_{a3} J_{22}^g(m, \omega_1, \omega_2) \varepsilon(p_2) \cdot \varepsilon^*(p_4) \quad (\text{A3})$$

with $\omega_1 = v \cdot p_2 - M$, $\omega_2 = v \cdot p_3 - M - \delta$;

$$\mathcal{M}_{(a4)}^{(2)} = \frac{-i g^2}{4 f^2} A_{a4} J_{22}^g(m, \omega_1, \omega_2) \varepsilon(p_2) \cdot \varepsilon^*(p_4) \quad (\text{A4})$$

with $\omega_1 = v \cdot p_1 - M - \delta$, $\omega_2 = v \cdot p_3 - M - \delta$;

$$\mathcal{M}_{(a5)}^{(2)} = \frac{i g^2}{4 f^2} A_{a5} J_{22}^g(m, \omega_1, \omega_2) \varepsilon(p_2) \cdot \varepsilon^*(p_4) \quad (\text{A5})$$

with $\omega_1 = v \cdot p_1 - M - \delta$, $\omega_2 = v \cdot p_4 - M$;

$$\mathcal{M}_{(a6)}^{(2)} = \frac{i g^2}{4 f^2} A_{a6} J_{22}^h(m, \omega_2, \omega_1) \varepsilon(p_2) \cdot \varepsilon^*(p_4) \quad (\text{A6})$$

with $\omega_1 = v \cdot p_1 - M - \delta$, $\omega_2 = v \cdot p_2 - M$;

$$\mathcal{M}_{(a7)}^{(2)} = \frac{i g^2}{4 f^2} A_{a7} J_{22}^h(m, \omega_2, \omega_1) \varepsilon(p_2) \cdot \varepsilon^*(p_4) \quad (\text{A7})$$

with $\omega_1 = v \cdot p_4 - M$, $\omega_2 = v \cdot p_3 - M - \delta$;

$$\mathcal{M}_{(a8)}^{(2)} = \frac{-i g^2}{2 f^2} A_{a8} J_{22}^h(m, \omega_2, \omega_1) \varepsilon(p_2) \cdot \varepsilon^*(p_4)$$

$$\text{with } \omega_1 = v \cdot p_1 - M - \delta, \omega_2 = v \cdot p_2 - M - \delta; \quad (\text{A8})$$

$$\mathcal{M}_{(a9)}^{(2)} = \frac{-i g^2}{2 f^2} A_{a9} J_{22}^h(m, \omega_2, \omega_1) \varepsilon(p_2) \cdot \varepsilon^*(p_4) \quad (\text{A9})$$

with $\omega_1 = v \cdot p_4 - M - \delta$, $\omega_2 = v \cdot p_3 - M - \delta$;

$$\mathcal{M}_{(a10)}^{(2)} = \frac{i g^2}{2 f^2} A_{a10} J_{22}^g(m, \omega_1, \omega_2) \varepsilon(p_2) \cdot \varepsilon^*(p_4) \quad (\text{A10})$$

with $\omega_1 = v \cdot p_2 - M - \delta$, $\omega_2 = v \cdot p_3 - M - \delta$;

$$\mathcal{M}_{(a11)}^{(2)} = \frac{i g^2}{2 f^2} A_{a11} J_{22}^g(m, \omega_1, \omega_2) \varepsilon(p_2) \cdot \varepsilon^*(p_4) \quad (\text{A11})$$

with $\omega_1 = v \cdot p_1 - M - \delta$, $\omega_2 = v \cdot p_4 - M - \delta$;

$$\begin{aligned} \mathcal{M}_{(a12+a13)}^{(2)} &= -i \frac{g^2}{f^2} A_{a12a13} \left(\frac{3}{8} \partial \omega J_{22}^b(m, \omega_1) + \frac{3}{4} \partial \omega J_{22}^b(m, \omega_2) \right) \\ &\quad \times \varepsilon(p_2) \cdot \varepsilon^*(p_4) \end{aligned}$$

with $\omega_1 = v \cdot p_2 - M$, $\omega_2 = v \cdot p_2 - M - \delta$, and with $\omega_1 = v \cdot p_4 - M$, $\omega_2 = v \cdot p_4 - M - \delta$;

$$\mathcal{M}_{(a14)}^{(2)} = -i \frac{g^2}{f^2} A_{a14} \left(\frac{9}{8} \partial \omega J_{22}^b(m, \omega_1) \right) \varepsilon(p_2) \cdot \varepsilon^*(p_4) \quad (\text{A12})$$

with $\omega_1 = v \cdot p_1 - M - \delta$, and with $\omega_1 = v \cdot p_3 - M - \delta$.

$$\begin{aligned} \mathcal{M}_{(a14)}^{(2)} &= -i \frac{g^2}{f^2} A_{a14} \left(\frac{9}{8} \partial \omega J_{22}^b(m, \omega_1) \right) \varepsilon(p_2) \cdot \varepsilon^*(p_4) \\ &\quad \text{with } \omega_1 = v \cdot p_1 - M - \delta, \text{ and with } \omega_1 = v \cdot p_3 - M - \delta. \end{aligned} \quad (\text{A13})$$

For the one-loop corrections to the OPE potentials in Fig. 4, the Feynman amplitudes are

$$\mathcal{M}_{(b1)}^{(2)} = \frac{i g^4}{4 f^4} A_{b1} \frac{p_\mu p_\nu}{p^2 - m^2} J_{22}^g(m, \omega_1, \omega_2) \varepsilon^\mu(p_2) \varepsilon^{*\nu}(p_4) \quad (\text{A14})$$

with $\omega_1 = v \cdot p_3 - M - \delta$, $\omega_2 = v \cdot p_2 - M$;

$$\mathcal{M}_{(b2)}^{(2)} = \frac{i g^4}{2 f^4} A_{b2} \frac{p_\mu p_\nu}{p^2 - m^2} J_{22}^g(m, \omega_1, \omega_2) \varepsilon^\mu(p_2) \varepsilon^{*\nu}(p_4) \quad (\text{A15})$$

with $\omega_1 = v \cdot p_2 - M - \delta$, $\omega_2 = v \cdot p_3 - M - \delta$;

$$\mathcal{M}_{(b3)}^{(2)} = \frac{i g^4}{4 f^4} A_{b3} \frac{p_\mu p_\nu}{p^2 - m^2} J_{22}^g(m, \omega_1, \omega_2) \varepsilon^\mu(p_2) \varepsilon^{*\nu}(p_4) \quad (\text{A16})$$

with $\omega_1 = v \cdot p_1 - M - \delta$, $\omega_2 = v \cdot p_4 - M$;

$$\mathcal{M}_{(b4)}^{(2)} = \frac{i g^4}{2 f^4} A_{b4} \frac{p_\mu p_\nu}{p^2 - m^2} J_{22}^g(m, \omega_1, \omega_2) \varepsilon^\mu(p_2) \varepsilon^{*\nu}(p_4) \quad (\text{A17})$$

with $\omega_1 = v \cdot p_1 - M - \delta$, $\omega_2 = v \cdot p_4 - M - \delta$;

$$\mathcal{M}_{(b5)}^{(2)} = i \frac{g^2}{f^4} A_{b5} \frac{p_\mu p_\nu}{p^2 - m^2} \left[2m^2 L + \frac{2m^2}{16\pi^2} \log\left(\frac{m}{\mu}\right) \right] \times \varepsilon^\mu(p_2) \varepsilon^{*\nu}(p_4); \quad (\text{A18})$$

$$\mathcal{M}_{(b6)}^{(2)} = i \frac{g^2}{f^4} A_{b6} \frac{p_\mu p_\nu}{p^2 - m^2} \left[2m^2 L + \frac{2m^2}{16\pi^2} \log\left(\frac{m}{\mu}\right) \right] \times \varepsilon^\mu(p_2) \varepsilon^{*\nu}(p_4); \quad (\text{A19})$$

$$\mathcal{M}_{(b7)}^{(2)} = i \frac{g^2}{f^2} A_{b7} \frac{p_\mu p_\nu}{p^2 - m^2} \left[\frac{2}{3f^2} \left(2m^2 L + \frac{2m^2}{16\pi^2} \log\left(\frac{m}{\mu}\right) \right) \right] \times \varepsilon^\mu(p_2) \varepsilon^{*\nu}(p_4); \quad (\text{A20})$$

$$\mathcal{M}_{(b8)}^{(2)} = 0; \quad \mathcal{M}_{(b9)}^{(2)} = 0; \quad (\text{A21})$$

$$\mathcal{M}_{(b10+b11)}^{(2)}$$

$$= -i \frac{g^4}{f^4} A_{b10b11} \frac{p_\mu p_\nu}{p^2 - m^2} \left(\frac{3}{8} \partial \omega J_{22}^b(m, \omega_1) + \frac{3}{4} \partial \omega J_{22}^b(m, \omega_2) \right) \times \varepsilon^\mu(p_2) \varepsilon^{*\nu}(p_4)$$

with $\omega_1 = v \cdot p_2 - M$, $\omega_2 = v \cdot p_2 - M - \delta$, and with $\omega_1 = v \cdot p_4 - M$, $\omega_2 = v \cdot p_4 - M - \delta$;

$$\mathcal{M}_{(b12)}^{(2)} = -i \frac{g^4}{f^4} A_{b12} \frac{p_\mu p_\nu}{p^2 - m^2} \left(\frac{9}{8} \partial \omega J_{22}^b(m, \omega_1) \right) \varepsilon^\mu(p_2) \varepsilon^{*\nu}(p_4) \quad (A22)$$

with $\omega_1 = v \cdot p_1 - M - \delta$, and with $\omega_1 = v \cdot p_3 - M - \delta$;

For the TPE potentials in Fig. 5, the Feynman amplitudes are

$$\mathcal{M}_{(c1)}^{(2)} = \frac{i}{4f^4} \left[4A_{c1a} (q_0^2 J_{21}^F + J_{22}^F) + 4A_{c1b} q_0^2 J_{11}^F + A_{c1c} J_0^F \right] \times \varepsilon(p_2) \cdot \varepsilon^*(p_4); \quad (A24)$$

$$\mathcal{M}_{(c2)}^{(2)} = \frac{-i}{4f^4} A_{c2} \left[(2A_{c2c} q_0 J_{31}^S + 2A_{c2c} J_{34}^S + A_{c2d} q_0 J_{21}^S) \times \varepsilon(p_2) \cdot \varepsilon^*(p_4) + (2A_{c2c} q_0 J_{32}^S + 2A_{c2c} J_{33}^S + (A_{c2d} + 2A_{c2c}) q_0 J_{22}^S + 2A_{c2c} J_{24}^S + A_{c2d} q_0 J_{11}^S) \times q \cdot \varepsilon(p_2) q \cdot \varepsilon^*(p_4) \right] \quad (A25)$$

with $\omega = v \cdot p_2 - M$;

$$\mathcal{M}_{(c3)}^{(2)} = \frac{i}{4f^4} A_{c3} \left[(2A_{c3d} q_0 J_{21}^S - (2A_{c3c} + A_{c3d}) q_0 \vec{q}^2 J_{22}^S - 2A_{c3c} \vec{q}^2 J_{24}^S + 4A_{c3c} q_0 J_{31}^S - 2A_{c3c} q_0 \vec{q}^2 J_{32}^S - 2A_{c3c} \vec{q}^2 J_{33}^S + 4A_{c3c} J_{34} - A_{c3d} q_0 \vec{q}^2 J_{11}^S) \varepsilon(p_2) \cdot \varepsilon^*(p_4) + (-A_{c3d} q_0 J_{11}^S - (2A_{c3c} + A_{c3d}) q_0 J_{22}^S - 2A_{c3c} J_{24}^S - 2A_{c3c} q_0 J_{32}^S - 2A_{c3c} J_{33}^S) q \cdot \varepsilon(p_2) q \cdot \varepsilon^*(p_4) \right] \quad (A26)$$

with $\omega = v \cdot p_2 - M - \delta$;

$$\mathcal{M}_{(c4)}^{(2)} = \frac{i}{4f^4} \left[A_{c4d} q_0 \vec{q}^2 J_{11}^T - 3A_{c4d} q_0 J_{21}^T + (2A_{c4c} + A_{c4d}) q_0 \vec{q}^2 J_{22}^T + 2A_{c4c} \vec{q}^2 J_{24}^T - 6A_{c4c} q_0 J_{31}^T + 2A_{c4c} q_0 \vec{q}^2 J_{32}^T + 2A_{c4c} \vec{q}^2 J_{33}^T - 6A_{c4c} J_{34}^T \right] \varepsilon(p_2) \cdot \varepsilon^*(p_4) \quad (A27)$$

with $\omega = v \cdot p_1 - M - \delta$;

$$\mathcal{M}_{(c5)}^{(2)} = \frac{i}{4f^4} A_{c5} \left[(-\vec{q}^2 J_{31}^B + 5J_{41}^B - \vec{q}^2 J_{42}^B) \varepsilon(p_2) \cdot \varepsilon^*(p_4) + (J_{21}^B - \vec{q}^2 J_{22}^B + 7J_{31}^B - 2\vec{q}^2 J_{32}^B + 7J_{42}^B - \vec{q}^2 J_{43}^B) \times q \cdot \varepsilon(p_2) q \cdot \varepsilon^*(p_4) \right]$$

$$\text{with } \omega_1 = v \cdot p_1 - M - \delta, \omega_2 = v \cdot p_2 - M; \quad (A28)$$

$$\mathcal{M}_{(c6)}^{(2)} = \frac{-i}{4f^4} A_{c6} \left[(-\vec{q}^2 J_{21}^B + (\vec{q}^2)^2 J_{22}^B - 9\vec{q}^2 J_{31}^B + 2(\vec{q}^2)^2 J_{32}^B + 10J_{41}^B - 9\vec{q}^2 J_{42}^B + (\vec{q}^2)^2 J_{43}^B) \varepsilon(p_2) \cdot \varepsilon^*(p_4) + (-J_{21}^B + \vec{q}^2 J_{22}^B - 7J_{31}^B + 2\vec{q}^2 J_{32}^B - 7J_{42}^B + \vec{q}^2 J_{43}^B) \times q \cdot \varepsilon(p_2) q \cdot \varepsilon^*(p_4) \right] \quad (A29)$$

with $\omega_1 = v \cdot p_1 - M - \delta$, $\omega_2 = v \cdot p_2 - M - \delta$;

$$\mathcal{M}_{(c7)}^{(2)} = \frac{-i}{4f^4} A_{c7} \left[\vec{p}^2 J_{21}^B \varepsilon(p_2) \cdot \varepsilon^*(p_4) + J_{21}^B p \cdot \varepsilon(p_2) p \cdot \varepsilon^*(p_4) \right] \quad (A30)$$

with $\omega_1 = v \cdot p_1 - M - \delta$, $\omega_2 = v \cdot p_2 - M - \delta$;

$$\mathcal{M}_{(c8)}^{(2)} = \frac{i}{4f^4} A_{c8} \left[(-\vec{q}^2 J_{31}^R + 5J_{41}^R - \vec{q}^2 J_{42}^R) \varepsilon(p_2) \cdot \varepsilon^*(p_4) + (J_{21}^R - \vec{q}^2 J_{22}^R + 7J_{31}^R - 2\vec{q}^2 J_{32}^R + 7J_{42}^R - \vec{q}^2 J_{43}^R) \times q \cdot \varepsilon(p_2) q \cdot \varepsilon^*(p_4) \right] \quad (A31)$$

with $\omega_1 = v \cdot p_1 - M - \delta$, $\omega_2 = v \cdot p_2$;

$$\mathcal{M}_{(c9)}^{(2)} = \frac{-i}{4f^4} A_{c9} \left[(-\vec{q}^2 J_{21}^R + (\vec{q}^2)^2 J_{22}^R - 9\vec{q}^2 J_{31}^R + 2(\vec{q}^2)^2 J_{32}^R + 10J_{41}^R - 9\vec{q}^2 J_{42}^R + (\vec{q}^2)^2 J_{43}^R) \varepsilon(p_2) \cdot \varepsilon^*(p_4) + (-J_{21}^R + \vec{q}^2 J_{22}^R - 7J_{31}^R + 2\vec{q}^2 J_{32}^R - 7J_{42}^R + \vec{q}^2 J_{43}^R) \times q \cdot \varepsilon(p_2) q \cdot \varepsilon^*(p_4) \right] \quad (A32)$$

with $\omega_1 = v \cdot p_1 - M - \delta$, $\omega_2 = v \cdot p_2 - M - \delta$;

$$\mathcal{M}_{(c10)}^{(2)} = \frac{i}{4f^4} A_{c10} \left[\vec{p}^2 J_{21}^R \varepsilon(p_2) \cdot \varepsilon^*(p_4) + J_{21}^R p \cdot \varepsilon(p_2) p \cdot \varepsilon^*(p_4) \right] \quad (A33)$$

with $\omega_1 = v \cdot p_1 - M - \delta$, $\omega_2 = v \cdot p_2 - M - \delta$;

In above, J_{ij}^F is the short notation for $J_{ij}^F(m_1, m_2, q)$, J_{ij}^S and J_{ij}^T are $J_{ij}^S(m_1, m_2, \omega, q)$ and $J_{ij}^T(m_1, m_2, \omega, q)$, respectively. J_{ij}^B and J_{ij}^R are $J_{ij}^B(m_1, m_2, \omega_1, \omega_2, q)$ and $J_{ij}^R(m_1, m_2, \omega_1, \omega_2, q)$, respectively. These loop functions like J^g are defined in the Appendix C.

In Eqs. (A1)–(A33), the constants A are different with different isospin. We list them in Tables I, II and III. The remaining constants are:

$$A_{c1b} = 1, \quad A_{c1c} = q_0^2, \quad A_{c2c} = -1, \quad A_{c2d} = -1, \quad A_{c3c} = -1, \quad A_{c3d} = -1, \quad A_{c4c} = 1, \quad A_{c4d} = 1, \quad (A34)$$

for $I = 1$. And

$$A_{c1b} = -3, \quad A_{c1c} = -3q_0^2, \quad A_{c2c} = 3, \quad A_{c2d} = 3, \quad A_{c3c} = 3, \quad A_{c3d} = 3, \quad A_{c4c} = -3, \quad A_{c4d} = -3, \quad (A35)$$

TABLE I: The coefficients for the contact amplitudes in the processes $DD^* \rightarrow DD^*$.

	$I = 1$	$I = 0$
A_{a1}	$-32D_a - 32E_a$	$-48D_a - 48E_a$
A_{a2}	$8D_b - 24D_a + 8E_a + 40E_b$	$24D_b - 24D_a - 24E_a + 24E_b$
A_{a3}	$-32D_b - 32E_b$	$48D_b + 48E_b$
A_{a4}	$16D_b - 80D_a - 16E_a + 80E_b$	$48D_b - 96D_a - 96E_a + 48E_b$
A_{a5}	$-32D_b - 32E_b$	$48D_b + 48E_b$
A_{a6}	$8D_a - 8D_b + 8E_a - 8E_b$	$24D_a + 24D_b - 72E_a - 72E_b$
A_{a7}	$8D_a - 8D_b + 8E_a - 8E_b$	$24D_a + 24D_b - 72E_a - 72E_b$
A_{a8}	0	$-48D_b + 144E_b$
A_{a9}	0	$-48D_b + 144E_b$
A_{a10}	$16D_b - 48E_b$	0
A_{a11}	$16D_b - 48E_b$	0
A_{a12a13}	$-8D_a + 8D_b - 8E_a + 8E_b$	$-8D_a - 8D_b + 24E_a + 24E_b$
A_{a14}	$-8D_a + 8D_b - 8E_a + 8E_b$	$-8D_a - 8D_b + 24E_a + 24E_b$

TABLE II: The coefficients for the OPE amplitudes in the processes $DD^* \rightarrow DD^*$.

	A_{b1}	A_{b2}	A_{b3}	A_{b4}	A_{b5}	A_{b6}	A_{b7}	A_f	A_{b10b11}	A_{b12}
$I = 1$	-1	1	-1	1	1/3	1/3	-1	-1	-1	-1
$I = 0$	-3	3	-3	3	1	1	-3	-3	-3	-3

TABLE III: The coefficients for the TPE amplitudes in the processes $DD^* \rightarrow DD^*$.

	A_{c1a}	A_{c2}	A_{c3}	A_{c4}	A_{c5}	A_{c6}	A_{c7}	A_{c8}	A_{c9}	A_{c10}
$I = 1$	1	-2	2	-2	1	-1	-1	5	-5	-5
$I = 0$	-3	-2	2	-2	9	-9	9	-3	3	-3

for $I = 0$.

In Eqs. (A1)-(A33), M is the D meson mass, δ is the mass difference between D^* and D , m, m_1, m_2 are all pion masses, $p = p_1 - p_4$, $q = p_1 - p_3$, μ is the renormalization scale in the dimensional regularization, and

$$L = \frac{1}{16\pi^2} \left(\frac{1}{d-4} + \frac{1}{2}(\gamma_E - 1 - \log 4\pi) \right). \quad (\text{A36})$$

Appendix B: Renormalized and bare couplings

We provide the relation between the renormalized coupling $g^{(2)}$ at experiment and the bare coupling g in the Lagrangian

$$g^{(2)} = g \left(1 - \frac{g^2}{2f^2} J_{22}^g(0, -\delta) + \frac{g^2}{4f^2} J_{22}^g(-\delta, \delta) - \frac{9g^2}{8f^2} \partial J_{22}^b(-\delta) - \frac{3g^2}{8f^2} \partial J_{22}^b(\delta) - \frac{3g^2}{4f^2} \partial J_{22}^b(0) \right). \quad (\text{B1})$$

The expression relating the renormalized $f_{(2)}$ and the bared f is well known

$$\frac{1}{f_{(2)}^2} = \frac{1}{f^2} \left(1 + \frac{m^2}{4\pi f^2} \log\left(\frac{m}{\mu}\right) \right). \quad (\text{B2})$$

We use $f_{(2)} = f_\pi = 0.092$ GeV.

Appendix C: Definitions of some loop functions

We define the loop functions following Ref. [84]:

$$i \int \frac{d^D l \mu^{4-D}}{(2\pi)^D} \frac{\{1, l^\alpha, l^\alpha l^\beta, l^\alpha l^\beta l^\gamma\}}{[(+/-)v \cdot l + \omega + i\varepsilon](l^2 - m^2 + i\varepsilon)} \\ \equiv \{J_0^{a/b}, v^\alpha J_{11}^{a/b}, v^\alpha v^\beta J_{21}^{a/b} + g^{\alpha\beta} J_{22}^{a/b}, (g \vee v) J_{31}^{a/b} + v^\alpha v^\beta v^\gamma J_{32}^{a/b}\}(m, \omega), \quad (\text{C1})$$

$$i \int \frac{d^D l \mu^{4-D}}{(2\pi)^D} \frac{\{1, l^\alpha, l^\alpha l^\beta, l^\alpha l^\beta l^\gamma\}}{(v \cdot l + \omega_1 + i\varepsilon)[(+/-)v \cdot l + \omega_2 + i\varepsilon](l^2 - m^2 + i\varepsilon)} \\ \equiv \{J_0^{g/h}, v^\alpha J_{11}^{g/h}, v^\alpha v^\beta J_{21}^{g/h} + g^{\alpha\beta} J_{22}^{g/h}, (g \vee v) J_{31}^{g/h} + v^\alpha v^\beta v^\gamma J_{32}^{g/h}\}(m, \omega_1, \omega_2), \quad (\text{C2})$$

$$i \int \frac{d^D l \mu^{4-D}}{(2\pi)^D} \frac{\{1, l^\alpha, l^\alpha l^\beta, l^\alpha l^\beta l^\gamma\}}{(l^2 - m_1^2 + i\varepsilon)[(q + l)^2 - m_2^2 + i\varepsilon]} \\ \equiv \{J_0^F, q^\alpha J_{11}^F, q^\alpha q^\beta J_{21}^F + g^{\alpha\beta} J_{22}^F, (g \vee q) J_{31}^F + q^\alpha q^\beta q^\gamma J_{32}^F\}(m_1, m_2, q), \quad (\text{C3})$$

$$i \int \frac{d^D l \mu^{4-D}}{(2\pi)^D} \frac{\{1, l^\alpha, l^\alpha l^\beta, l^\alpha l^\beta l^\gamma, l^\alpha l^\beta l^\gamma l^\delta\}}{[(+/-)v \cdot l + \omega + i\varepsilon](l^2 - m_1^2 + i\varepsilon)[(q + l)^2 - m_2^2 + i\varepsilon]} \\ \equiv \{J_0^{T/S}, q^\alpha J_{11}^{T/S} + v^\alpha J_{12}^{T/S}, g^{\alpha\beta} J_{21}^{T/S} + q^\alpha q^\beta J_{22}^{T/S} + v^\alpha v^\beta J_{23}^{T/S} + (q \vee v) J_{24}^{T/S}, (g \vee q) J_{31}^{T/S} + q^\alpha q^\beta q^\gamma J_{32}^{T/S} + (q^2 \vee v) J_{33}^{T/S} \\ + (g \vee v) J_{34}^{T/S} + (q \vee v^2) J_{35}^{T/S} + v^\alpha v^\beta v^\gamma J_{36}^{T/S}, (g \vee g) J_{41}^{T/S} + (g \vee q^2) J_{42}^{T/S} + q^\alpha q^\beta q^\gamma q^\delta J_{43}^{T/S} + (g \vee v^2) J_{44}^{T/S} + v^\alpha v^\beta v^\gamma v^\delta J_{45}^{T/S} \\ + (q^3 \vee v) J_{46}^{T/S} + (q^2 \vee v^2) J_{47}^{T/S} + (q \vee v^3) J_{48}^{T/S} + (g \vee q \vee v) J_{49}^{T/S}\}(m_1, m_2, \omega, q), \quad (\text{C4})$$

$$i \int \frac{d^D l \mu^{4-D}}{(2\pi)^D} \frac{\{1, l^\alpha, l^\alpha l^\beta, l^\alpha l^\beta l^\gamma, l^\alpha l^\beta l^\gamma l^\delta\}}{(v \cdot l + \omega_1 + i\varepsilon)[(+/-)v \cdot l + \omega_2 + i\varepsilon](l^2 - m_1^2 + i\varepsilon)[(q + l)^2 - m_2^2 + i\varepsilon]}$$

$$\begin{aligned}
&\equiv \left\{ J_0^{R/B}, q^\alpha J_{11}^{R/B} + v^\alpha J_{12}^{R/B}, g^{\alpha\beta} J_{21}^{R/B} + q^\alpha q^\beta J_{22}^{R/B} + v^\alpha v^\beta J_{23}^{R/B} + (q \vee v) J_{24}^{R/B}, (g \vee q) J_{31}^{R/B} + q^\alpha q^\beta q^\gamma J_{32}^{R/B} + (q^2 \vee v) J_{33}^{R/B} \right. \\
&+ (g \vee v) J_{34}^{R/B} + (q \vee v^2) J_{35}^{R/B} + v^\alpha v^\beta v^\gamma J_{36}^{R/B}, (g \vee g) J_{41}^{R/B} + (g \vee q^2) J_{42}^{R/B} + q^\alpha q^\beta q^\gamma q^\delta J_{43}^{R/B} + (g \vee v^2) J_{44}^{R/B} + v^\alpha v^\beta v^\gamma v^\delta J_{45}^{R/B} \\
&\left. + (q^3 \vee v) J_{46}^{R/B} + (q^2 \vee v^2) J_{47}^{R/B} + (q \vee v^3) J_{48}^{R/B} + (g \vee q \vee v) J_{49}^{R/B} \right\} (m_1, m_2, \omega_1, \omega_2, q), \quad (C5)
\end{aligned}$$

with

$$\begin{aligned}
q \vee v &\equiv q^\alpha v^\beta + q^\beta v^\alpha, \quad g \vee q \equiv g^{\alpha\beta} q^\gamma + g^{\alpha\gamma} q^\beta + g^{\gamma\beta} q^\alpha, \quad g \vee v \equiv g^{\alpha\beta} v^\gamma + g^{\alpha\gamma} v^\beta + g^{\gamma\beta} v^\alpha, \\
q^2 \vee v &\equiv q^\beta q^\gamma v^\alpha + q^\alpha q^\gamma v^\beta + q^\alpha q^\beta v^\gamma, \quad q \vee v^2 \equiv q^\gamma v^\alpha v^\beta + q^\beta v^\alpha v^\gamma + q^\alpha v^\beta v^\gamma, \\
g \vee g &\equiv g^{\alpha\beta} g^{\gamma\delta} + g^{\alpha\delta} g^{\beta\gamma} + g^{\alpha\gamma} g^{\beta\delta}, \quad g \vee q^2 \equiv q^\alpha q^\beta g^{\gamma\delta} + q^\alpha q^\delta g^{\beta\gamma} + q^\alpha q^\gamma g^{\beta\delta} + q^\gamma q^\delta g^{\alpha\beta} + q^\beta q^\delta g^{\alpha\gamma} + q^\beta q^\gamma g^{\alpha\delta}, \\
g \vee v^2 &\equiv v^\alpha v^\beta g^{\gamma\delta} + v^\alpha v^\delta g^{\beta\gamma} + v^\alpha v^\gamma g^{\beta\delta} + v^\gamma v^\delta g^{\alpha\beta} + v^\beta v^\delta g^{\alpha\gamma} + v^\beta v^\gamma g^{\alpha\delta}, \\
q^3 \vee v &\equiv q^\beta q^\gamma q^\delta v^\alpha + q^\alpha q^\gamma q^\delta v^\beta + q^\alpha q^\beta q^\delta v^\gamma + q^\alpha q^\beta q^\gamma v^\delta, \quad q \vee v^3 \equiv q^\delta v^\alpha v^\beta v^\gamma + q^\gamma v^\alpha v^\beta v^\delta + q^\beta v^\alpha v^\gamma v^\delta + q^\alpha v^\beta v^\gamma v^\delta, \\
q^2 \vee v^2 &\equiv q^\gamma q^\delta v^\alpha v^\beta + q^\beta q^\delta v^\alpha v^\gamma + q^\alpha q^\delta v^\beta v^\gamma + q^\beta q^\gamma v^\alpha v^\delta + q^\alpha q^\gamma v^\beta v^\delta + q^\alpha q^\beta v^\gamma v^\delta, \\
g \vee q \vee v &\equiv q^\beta v^\alpha g^{\gamma\delta} + q^\alpha v^\beta g^{\gamma\delta} + q^\delta v^\alpha g^{\beta\gamma} + q^\gamma v^\alpha g^{\beta\delta} + q^\alpha v^\delta g^{\beta\gamma} + q^\alpha v^\gamma g^{\beta\delta} + q^\delta v^\gamma g^{\alpha\beta} + q^\delta v^\beta g^{\alpha\gamma} + q^\gamma v^\delta g^{\alpha\beta} \\
&+ q^\gamma v^\beta g^{\alpha\delta} + q^\beta v^\delta g^{\alpha\gamma} + q^\beta v^\gamma g^{\alpha\delta}. \quad (C6)
\end{aligned}$$

J^b is related to J^a :

$$\begin{aligned}
J_0^b &= J_0^a, \quad J_{11}^b = -J_{11}^a, \quad J_{21}^b = J_{21}^a, \quad J_{22}^b = J_{22}^a, \\
J_{31}^b &= -J_{31}^a, \quad J_{32}^b = -J_{32}^a. \quad (C7)
\end{aligned}$$

J^g and J^h can be deduced to

$$J^g(\omega_1, \omega_2) = \frac{1}{\omega_2 - \omega_1} [J^a(\omega_1) - J^a(\omega_2)], \quad (C8)$$

$$J^h(\omega_1, \omega_2) = \frac{1}{\omega_2 + \omega_1} [J^a(\omega_1) + J^b(\omega_2)]. \quad (C9)$$

J^S is related to J^T :

$$\begin{aligned}
J_0^S(v \cdot q) &= J_0^T(-v \cdot q), \quad J_{11}^S(v \cdot q) = J_{11}^T(-v \cdot q), \\
J_{12}^S(v \cdot q) &= -J_{12}^T(-v \cdot q), \quad J_{21}^S = J_{21}^T(-v \cdot q), \\
J_{22}^S(v \cdot q) &= J_{22}^T(-v \cdot q), \quad J_{23}^S(v \cdot q) = J_{23}^T(-v \cdot q), \\
J_{24}^S(v \cdot q) &= -J_{24}^T(-v \cdot q), \quad J_{31}^S(v \cdot q) = J_{31}^T(-v \cdot q), \\
J_{32}^S(v \cdot q) &= J_{32}^T(-v \cdot q), \quad J_{33}^S(v \cdot q) = -J_{33}^T(-v \cdot q), \\
J_{34}^S(v \cdot q) &= -J_{34}^T(-v \cdot q), \quad J_{35}^S(v \cdot q) = J_{35}^T(-v \cdot q), \\
J_{36}^S(v \cdot q) &= -J_{36}^T(-v \cdot q), \quad J_{41}^S(v \cdot q) = J_{41}^T(-v \cdot q), \\
J_{42}^S(v \cdot q) &= J_{42}^T(-v \cdot q), \quad J_{43}^S(v \cdot q) = J_{43}^T(-v \cdot q), \\
J_{44}^S(v \cdot q) &= J_{44}^T(-v \cdot q), \quad J_{45}^S(v \cdot q) = J_{45}^T(-v \cdot q), \\
J_{46}^S(v \cdot q) &= -J_{46}^T(-v \cdot q), \quad J_{47}^S(v \cdot q) = J_{47}^T(-v \cdot q), \\
J_{48}^S(v \cdot q) &= -J_{48}^T(-v \cdot q), \quad J_{49}^S(v \cdot q) = -J_{49}^T(-v \cdot q). \quad (C10)
\end{aligned}$$

J^R and J^B can be deduced to

$$J^R(\omega_1, \omega_2) = \frac{1}{\omega_2 - \omega_1} [J^T(\omega_1) - J^T(\omega_2)], \quad (C11)$$

$$J^B(\omega_1, \omega_2) = \frac{1}{\omega_2 + \omega_1} [J^T(\omega_1) + J^S(\omega_2)]. \quad (C12)$$

All the integrals in Eqs. (C1)-(C5) can be deduced to one or two dimensional Feynmann parameter integrals without difficulty. For example,

$$J_{36}^T$$

$$\begin{aligned}
&= 2L \int_0^1 dx_1 (4b^2 - c) + \frac{3}{16\pi^2} \int_0^1 dx_1 b^2 + \frac{1}{16\pi^2} \int_0^1 dx_1 \\
&\times (4b^2 - c) [-\log \mu^2 + \log(-b^2 + c)] - \frac{3}{16\pi} \int_0^1 dx_1 b \\
&\times (-b^2 + c)^{\frac{1}{2}} + \frac{1}{16\pi} \int_0^1 dx_1 b^3 (-b^2 + c)^{-\frac{1}{2}} \\
&- \frac{1}{8\pi^2} \int_0^1 dx_1 D, \quad (C13)
\end{aligned}$$

$$\begin{aligned}
&J_{45}^T \\
&= 8L \int_0^1 dx_1 b (2b^2 - c) + \frac{1}{4\pi^2} \int_0^1 dx_1 b^3 + \frac{1}{4\pi^2} \int_0^1 dx_1 \\
&\times b (2b^2 - c) [-\log \mu^2 + \log(-b^2 + c)] + \frac{1}{16\pi} \int_0^1 dx_1 \\
&\times (-b^2 + c)^{\frac{3}{2}} - \frac{3}{8\pi} \int_0^1 dx_1 b^2 (-b^2 + c)^{\frac{1}{2}} + \frac{1}{16\pi} \int_0^1 dx_1 \\
&\times b^4 (-b^2 + c)^{-\frac{1}{2}} + \frac{1}{8\pi^2} \int_0^1 dx_1 E, \quad (C14)
\end{aligned}$$

where

$$\begin{aligned}
b &= (1 - x_1)v \cdot q - \omega, \\
c &= (1 - x_1)^2 q^2 - (1 - x_1)q^2 + x_1(m_1^2 - m_2^2) + m_2^2 - i\epsilon, \\
D &= \left\{ \sqrt{c - b^2} \left[(4b^2 - c) \log \left(1 - \frac{b^2}{c} \right) + 5b^2 \right] + (8b^3 - 6bc) \right. \\
&\times \tan^{-1} \left(\frac{b}{\sqrt{c - b^2}} \right) \left. \right\} (2\sqrt{c - b^2})^{-1}, \\
E &= \left\{ b\sqrt{c - b^2} \left[6(2b^2 - c) \left(\log(c) - \log[c - b^2] \right) - 16b^2 \right. \right. \\
&+ 3c \left. \right] - 3(8b^4 - 8b^2c + c^2) \tan^{-1} \left(\frac{b}{\sqrt{c - b^2}} \right) \left. \right\} \\
&\times (3\sqrt{c - b^2})^{-1},
\end{aligned}$$

(C15)

and L is defined in Eq. (A36).

One should notice that in Eqs. (C1)-(C5), if the form of the integral Eq. (16) is encountered, the 2PR part must be subtracted using Eq. (17).

However, the evaluations of above loop integrals are not complete since the kinetic energy terms in the propagators are not included. Here, we further illustrate the calculations con-

sidering the kinetic energy terms $\frac{q^2}{2M}$. We choose J_0^b as an example,

$$i \int \frac{d^D l \mu^{4-D}}{(2\pi)^D} \frac{1}{\left[-v \cdot l - \frac{(\vec{p}-\vec{l})^2}{2M} + \omega + i\varepsilon \right] [l^2 - m^2 + i\varepsilon]}. \quad (C16)$$

We first apply the Feynman parametrization to Eq. (C16):

$$\begin{aligned} \frac{1}{\left[-v \cdot l - \frac{(\vec{p}-\vec{l})^2}{2M} + \omega + i\varepsilon \right] [l^2 - m^2 + i\varepsilon]} &= 2 \int_0^\infty dy \frac{1}{\left[l^2 - m^2 + 2y \left(-v \cdot l - \frac{(\vec{p}-\vec{l})^2}{2M} + \omega \right) + i\varepsilon \right]^2} \\ &= 2 \int_0^\infty dy \frac{1}{\left[l^2 - 2yv \cdot l + y^2 v^2 - y^2 v^2 - \frac{y}{M} (\vec{p} - \vec{l})^2 + 2y\omega - m^2 + i\varepsilon \right]^2} \\ &= 2 \int_0^\infty dy \frac{1}{\left[(l - yv)^2 - y^2 - \frac{y}{M} (\vec{p} - \vec{l})^2 + 2y\omega - m^2 + i\varepsilon \right]^2}. \end{aligned} \quad (C17)$$

with the substitution $l \rightarrow l + yv$ we obtain

$$2 \int_0^\infty dy \frac{1}{\left[l^2 - y^2 - \frac{y}{M} (\vec{p} - \vec{l})^2 + 2y\omega - m^2 + i\varepsilon \right]^2}. \quad (C18)$$

Next, we analyze the pole structure of the expression and perform l_0 integral. We first rewrite the polynomial of l_0 in the denominator:

$$\begin{aligned} l^2 - y^2 - \frac{y}{M} (\vec{p} - \vec{l})^2 + 2y\omega - m^2 + i\varepsilon \\ = l_0^2 - \vec{l}^2 - y^2 - \frac{y}{M} (\vec{p} - \vec{l})^2 + 2y\omega - m^2 + i\varepsilon \\ = l_0^2 - \left[\vec{l}^2 + \frac{y}{M} (\vec{p} - \vec{l})^2 + y^2 - 2y\omega + m^2 \right] + i\varepsilon \\ = [l_0 + E_l][l_0 - E_l], \end{aligned} \quad (C19)$$

where $E_l = \sqrt{\vec{l}^2 + \frac{y}{M} (\vec{p} - \vec{l})^2 + y^2 - 2y\omega + m^2 - i\varepsilon}$. Therefore there exist two poles located at $-E_l$ and E_l .

With the expressions above, Eq. (C16) becomes

$$\begin{aligned} i \int \frac{d^D l \mu^{4-D}}{(2\pi)^D} \frac{1}{\left[-v \cdot l - \frac{(\vec{p}-\vec{l})^2}{2M} + \omega + i\varepsilon \right] [l^2 - m^2 + i\varepsilon]} \\ = 2i \int_0^\infty dy \int \frac{d^D l \mu^{4-D}}{(2\pi)^D} \frac{1}{[l_0 + E_l]^2 [l_0 - E_l]^2} \\ = 2i \int_0^\infty dy \int \frac{d^{D-1} l \mu^{4-D}}{(2\pi)^D} \int dl_0 \frac{1}{[l_0 + E_l]^2 [l_0 - E_l]^2}. \end{aligned} \quad (C20)$$

By closing the contour in the upper complex l_0 plane, we obtain the l_0 integral

$$\int dl_0 \frac{1}{[l_0 + E_l]^2 [l_0 - E_l]^2} = 2\pi i \text{Res}(f(-E_l)), \quad (C21)$$

where $\text{Res}(f(-E_l))$ is the residue at $-E_l$, it can be evaluated using

$$\text{Res}(f(z_0)) = \lim_{z \rightarrow z_0} \frac{1}{(m-1)!} \left\{ \frac{d^{m-1}}{dz^{m-1}} [(z - z_0)^m f(z)] \right\}, \quad (C22)$$

i.e.,

$$\begin{aligned} \text{Res}(f(-E_l)) &= \lim_{l_0 \rightarrow -E_l} \left\{ \frac{d}{dl_0} \left[(l_0 - (-E_l))^2 \frac{1}{[l_0 + E_l]^2 [l_0 - E_l]^2} \right] \right\} \\ &= \lim_{l_0 \rightarrow -E_l} \frac{2}{(E_l - l_0)^3} \\ &= \frac{2}{(2E_l)^3} \\ &= \frac{1}{4} \frac{1}{\left[\vec{l}^2 + \frac{y}{M} (\vec{p} - \vec{l})^2 + y^2 - 2y\omega + m^2 - i\varepsilon \right]^{3/2}}, \end{aligned} \quad (C23)$$

where the expression $\vec{l}^2 + \frac{y}{M} (\vec{p} - \vec{l})^2 + y^2 - 2y\omega + m^2 - i\varepsilon$ should be further simplified:

$$\begin{aligned} \left(1 + \frac{y}{M} \right) \left[\vec{l}^2 - \frac{\frac{y}{M}}{1 + \frac{y}{M}} \vec{p} \right]^2 + \frac{\frac{y}{M}}{1 + \frac{y}{M}} \vec{p}^2 + (y - \omega)^2 + m^2 - \omega^2 \\ = \left(1 + \frac{y}{M} \right) \vec{l}^2 + (y - \omega)^2 + m^2 - \omega^2 \\ = \left(1 + \frac{y}{M} \right) \left[\vec{l}^2 + \frac{(y - \omega)^2 + m^2 - \omega^2}{1 + \frac{y}{M}} \right] \\ = \left(1 + \frac{y}{M} \right) [\vec{l}^2 + \Delta] \end{aligned} \quad (C24)$$

with

$$\Delta = \frac{(y - \omega)^2 + m^2 - \omega^2}{1 + \frac{y}{M}}. \quad (C25)$$

Then, Eq. (C20) reduces to

$$\begin{aligned}
& 2i \int_0^\infty dy \int \frac{d^{D-1} l \mu^{4-D}}{(2\pi)^D} (2\pi i) \frac{1}{4} \frac{1}{\left[\left(1 + \frac{y}{M}\right) [\vec{l}^2 + \Delta] \right]^{3/2}} \\
&= -\frac{1}{2} \int_0^\infty dy \int \frac{d^{D-1} l \mu^{4-D}}{(2\pi)^{D-1}} \frac{1}{\left[\left(1 + \frac{y}{M}\right) [\vec{l}^2 + \Delta] \right]^{3/2}} \\
&= -\frac{1}{2} \int_0^\infty dy \frac{\mu^{4-D}}{(2\pi)^{\frac{D-1}{2}}} \frac{\Gamma[2 - \frac{D}{2}]}{\Gamma[\frac{3}{2}]} \frac{1}{\left(1 + \frac{y}{M}\right) \Delta^{2 - \frac{D}{2}}}. \quad (\text{C26})
\end{aligned}$$

Using

$$y \rightarrow y + \omega, \quad \Delta \rightarrow \frac{y^2 + m^2 - \omega^2}{1 + \frac{y+\omega}{M}}, \quad (\text{C27})$$

Eq. (C26) can be further simplified

$$\begin{aligned}
& -\frac{1}{2} \int_{-\omega}^\infty dy \frac{\mu^{4-D}}{(2\pi)^{\frac{D-1}{2}}} \frac{\Gamma[2 - \frac{D}{2}]}{\Gamma[\frac{3}{2}]} \frac{1}{\left(1 + \frac{y+\omega}{M}\right)^{3/2} \Delta^{2 - \frac{D}{2}}} \\
&= -\frac{1}{2} \int_{-\omega}^\infty dy \frac{\mu^\epsilon}{(2\pi)^{\frac{3-\epsilon}{2}}} \frac{\Gamma[\frac{\epsilon}{2}]}{\Gamma[\frac{3}{2}]} \frac{1}{\left(1 + \frac{y+\omega}{M}\right)^{3/2} \Delta^{\frac{\epsilon}{2}}} \\
&= -\frac{1}{2} \int_0^\infty dy \frac{\mu^\epsilon}{(2\pi)^{\frac{3-\epsilon}{2}}} \frac{\Gamma[\frac{\epsilon}{2}]}{\Gamma[\frac{3}{2}]} \frac{1}{\left(1 + \frac{y+\omega}{M}\right)^{3/2} \Delta^{\frac{\epsilon}{2}}} \\
&+ \frac{-1}{2} \int_{-\omega}^0 dy \frac{\mu^\epsilon}{(2\pi)^{\frac{3-\epsilon}{2}}} \frac{\Gamma[\frac{\epsilon}{2}]}{\Gamma[\frac{3}{2}]} \frac{1}{\left(1 + \frac{y+\omega}{M}\right)^{3/2} \Delta^{\frac{\epsilon}{2}}}, \quad (\text{C28})
\end{aligned}$$

where $\epsilon = 4 - D$.

We first discuss the \int_0^∞ part,

$$\begin{aligned}
& -\frac{1}{2} \int_0^\infty dy \frac{\mu^\epsilon}{(2\pi)^{\frac{3-\epsilon}{2}}} \frac{\Gamma[\frac{\epsilon}{2}]}{\Gamma[\frac{3}{2}]} \frac{1}{\left(1 + \frac{y+\omega}{M}\right)^{3/2} \Delta^{\frac{\epsilon}{2}}} \\
&= -\frac{1}{2} \frac{(4\pi)^{\frac{1}{2}}}{\Gamma[\frac{3}{2}]} \frac{\mu^\epsilon \Gamma[\frac{\epsilon}{2}]}{(4\pi)^{2-\frac{\epsilon}{2}}} \int_0^\infty dy \frac{\left(1 + \frac{y+\omega}{M}\right)^{-\frac{3}{2}}}{\left(\frac{y^2 - \omega^2 + m^2}{1 + \frac{y+\omega}{M}}\right)^{\frac{\epsilon}{2}}} \\
&= -\frac{1}{2} \frac{(4\pi)^{\frac{1}{2}}}{\Gamma[\frac{3}{2}]} \frac{\mu^\epsilon \Gamma[\frac{\epsilon}{2}]}{(4\pi)^{2-\frac{\epsilon}{2}}} \int_0^\infty dy \frac{\left(1 + \frac{y+\omega}{M}\right)^{-\frac{3}{2}}}{(y^2 - \omega^2 + m^2)^{\frac{\epsilon}{2}}}. \quad (\text{C29})
\end{aligned}$$

Notice that, if we assume $M \rightarrow \infty$, the expression above becomes

$$\begin{aligned}
& -\frac{1}{2} \frac{(4\pi)^{\frac{1}{2}}}{\Gamma[\frac{3}{2}]} \frac{\mu^\epsilon \Gamma[\frac{\epsilon}{2}]}{(4\pi)^{2-\frac{\epsilon}{2}}} \int_0^\infty dy \frac{1}{(y^2 - \omega^2 + m^2)^{\frac{\epsilon}{2}}} \\
&= -2 \frac{\mu^\epsilon \Gamma[\frac{\epsilon}{2}]}{(4\pi)^{2-\frac{\epsilon}{2}}} \frac{\Gamma[\frac{1}{2}] \Gamma[\frac{-1}{2}]}{2\Gamma[\frac{\epsilon}{2}]} (-\omega^2 + m^2)^{\frac{1}{2}-\frac{\epsilon}{2}} \\
&= \frac{1}{8\pi} (-\omega^2 + m^2)^{\frac{1}{2}}. \quad (\text{C30})
\end{aligned}$$

The result above reproduces part of J_0^b where \vec{q}^2/M in the propagator is not included.

We now discuss the $\int_{-\omega}^0$ part:

$$\begin{aligned}
& -\frac{1}{2} \int_{-\omega}^0 dy \frac{\mu^\epsilon}{(2\pi)^{\frac{3-\epsilon}{2}}} \frac{\Gamma[\frac{\epsilon}{2}]}{\Gamma[\frac{3}{2}]} \frac{1}{\left(1 + \frac{y+\omega}{M}\right)^{3/2} \Delta^{\frac{\epsilon}{2}}} \\
&= -\frac{1}{2} \frac{(4\pi)^{\frac{1}{2}}}{\Gamma[\frac{3}{2}]} \frac{\mu^\epsilon \Gamma[\frac{\epsilon}{2}]}{(4\pi)^{2-\frac{\epsilon}{2}}} \int_{-\omega}^0 dy \frac{\left(1 + \frac{y+\omega}{M}\right)^{-\frac{3}{2}}}{(y^2 - \omega^2 + m^2)^{\frac{\epsilon}{2}}} \\
&= -2 \left(-2L + \frac{1}{8\pi^2} \log \mu - \frac{1}{16\pi^2} \right) \int_{-\omega}^0 dy \left(1 + \frac{y+\omega}{M}\right)^{-\frac{3}{2}} \\
&\quad \times \frac{\left(1 + \frac{y+\omega}{M}\right)^{\frac{\epsilon}{2}}}{(y^2 - \omega^2 + m^2)^{\frac{\epsilon}{2}}} \\
&= -2 \left(-2L + \frac{1}{8\pi^2} \log \mu - \frac{1}{16\pi^2} \right) \int_{-\omega}^0 dy \left(1 + \frac{y+\omega}{M}\right)^{-\frac{3}{2}} \\
&\quad \times \left[1 + \frac{\epsilon}{2} \log \frac{1 + \frac{y+\omega}{M}}{y^2 - \omega^2 + m^2} \right] \\
&= \left(4L - \frac{1}{4\pi^2} \log \mu + \frac{1}{8\pi^2} \right) \int_{-\omega}^0 dy \left(1 + \frac{y+\omega}{M}\right)^{-\frac{3}{2}} \\
&\quad - \frac{1}{8\pi^2} \int_{-\omega}^0 dy \left(1 + \frac{y+\omega}{M}\right)^{-\frac{3}{2}} \log \frac{1 + \frac{y+\omega}{M}}{y^2 - \omega^2 + m^2}, \quad (\text{C31})
\end{aligned}$$

where the term containing L (defined in Eq. (A36)) is a divergent part. The expression above will be further evaluated numerically. If we assume $M \rightarrow \infty$ again, the result can reproduce another part of J_0^b where \vec{q}^2/M in the propagator is not included at the beginning.

The evaluations of other loop integrals in Eqs. (C1)-(C5) are similar.

- [1] S. Weinberg, Phenomenological Lagrangians, *Physica A* **96**, 327 (1979).
[2] J. Gasser and H. Leutwyler, Chiral Perturbation Theory to One Loop, *Annals Phys.* **158**, 142 (1984).

- [3] S. Scherer and M. R. Schindler, A Primer for Chiral Perturbation Theory (Springer-Verlag, Berlin, 2012), Vol. 830, p. 1.
[4] E. E. Jenkins and A. V. Manohar, Baryon chiral perturbation theory using a heavy fermion Lagrangian,

- Phys. Lett. B **255**, 558 (1991).
- [5] V. Bernard, N. Kaiser, J. Kambor and U. G. Meissner, Chiral structure of the nucleon, *Nucl. Phys. B* **388**, 315 (1992).
 - [6] V. Bernard, N. Kaiser and U. G. Meissner, Chiral dynamics in nucleons and nuclei, *Int. J. Mod. Phys. E* **4**, 193 (1995).
 - [7] T. Becher and H. Leutwyler, Baryon chiral perturbation theory in manifestly Lorentz invariant form, *Eur. Phys. J. C* **9**, 643 (1999).
 - [8] T. Fuchs, J. Gegelia, G. Japaridze and S. Scherer, Renormalization of relativistic baryon chiral perturbation theory and power counting, *Phys. Rev. D* **68**, 056005 (2003).
 - [9] L. Geng, Recent developments in SU(3) covariant baryon chiral perturbation theory, *Front. Phys. (Beijing)* **8**, 328 (2013).
 - [10] F. K. Guo, C. Hanhart and U. G. Meissner, Interactions between heavy mesons and Goldstone bosons from chiral dynamics, *Eur. Phys. J. A* **40**, 171 (2009).
 - [11] Y. R. Liu, X. Liu and S. L. Zhu, Light Pseudoscalar Meson and Heavy Meson Scattering Lengths, *Phys. Rev. D* **79**, 094026 (2009).
 - [12] L. S. Geng, N. Kaiser, J. Martin-Camalich and W. Weise, Low-energy interactions of Nambu-Goldstone bosons with D mesons in covariant chiral perturbation theory, *Phys. Rev. D* **82**, 054022 (2010).
 - [13] P. Wang and X. G. Wang, Study on 0^+ states with open charm in unitarized heavy meson chiral approach, *Phys. Rev. D* **86**, 014030 (2012).
 - [14] M. Altenbuchinger, L.-S. Geng and W. Weise, Scattering lengths of Nambu-Goldstone bosons off D mesons and dynamically generated heavy-light mesons, *Phys. Rev. D* **89**, no. 1, 014026 (2014).
 - [15] Z. H. Guo, U. G. Meiner and D. L. Yao, New insights into the D_{s0}^* (2317) and other charm scalar mesons, *Phys. Rev. D* **92**, 094008 (2015).
 - [16] D. L. Yao, M. L. Du, F. K. Guo and U. G. Meiner, One-loop analysis of the interactions between charmed mesons and Goldstone bosons, *JHEP* **1511**, 058 (2015).
 - [17] M. L. Du, F. K. Guo, U. G. Meiner and D. L. Yao, Study of open-charm 0^+ states in unitarized chiral effective theory with one-loop potentials, [arXiv:1703.10836 \[hep-ph\]](#).
 - [18] M. L. Du, F. K. Guo and U. G. Meissner, Subtraction of power counting breaking terms in chiral perturbation theory: spinless matter fields, *JHEP* **1610**, 122 (2016).
 - [19] S. Weinberg, Nuclear forces from chiral Lagrangians, *Phys. Lett. B* **251**, 288 (1990).
 - [20] S. Weinberg, Effective chiral Lagrangians for nucleon - pion interactions and nuclear forces, *Nucl. Phys. B* **363**, 3 (1991).
 - [21] C. Ordonez and U. van Kolck, Chiral lagrangians and nuclear forces, *Phys. Lett. B* **291**, 459 (1992).
 - [22] C. Ordonez, L. Ray and U. van Kolck, The Two nucleon potential from chiral Lagrangians, *Phys. Rev. C* **53**, 2086 (1996).
 - [23] E. Epelbaum, W. Gloeckle and U. G. Meissner, Nuclear forces from chiral Lagrangians using the method of unitary transformation. 1. Formalism, *Nucl. Phys. A* **637**, 107 (1998).
 - [24] E. Epelbaum, W. Gloeckle and U. G. Meissner, Nuclear forces from chiral Lagrangians using the method of unitary transformation. 2. The two nucleon system, *Nucl. Phys. A* **671**, 295 (2000).
 - [25] M. P. Valderrama, Perturbative renormalizability of chiral two pion exchange in nucleon-nucleon scattering, *Phys. Rev. C* **83**, 024003 (2011).
 - [26] M. Pavon Valderrama, Perturbative Renormalizability of Chiral Two Pion Exchange in Nucleon-Nucleon Scattering: P- and D-waves, *Phys. Rev. C* **84**, 064002 (2011).
 - [27] B. Long and C. J. Yang, Renormalizing chiral nuclear forces: a case study of 3P_0 , *Phys. Rev. C* **84**, 057001 (2011).
 - [28] B. Long and C. J. Yang, Short-range nuclear forces in singlet channels, *Phys. Rev. C* **86**, 024001 (2012).
 - [29] B. Long and Y. Mei, Cutoff regulators in chiral nuclear effective field theory, *Phys. Rev. C* **93**, no. 4, 044003 (2016).
 - [30] E. Epelbaum, H. Krebs and U. G. Meiner, Improved chiral nucleon-nucleon potential up to next-to-next-to-next-to-leading order, *Eur. Phys. J. A* **51**, no. 5, 53 (2015).
 - [31] X. W. Kang, J. Haidenbauer and U. G. Meiner, Antinucleon-nucleon interaction in chiral effective field theory, *JHEP* **1402**, 113 (2014).
 - [32] L. Y. Dai, J. Haidenbauer and U. G. Meiner, Antinucleon-nucleon interaction at next-to-next-to-next-to-leading order in chiral effective field theory, [arXiv:1702.02065 \[nucl-th\]](#).
 - [33] X. L. Ren, K. W. Li, L. S. Geng, B. W. Long, P. Ring and J. Meng, Leading order covariant chiral nucleon-nucleon interaction, [arXiv:1611.08475 \[nucl-th\]](#).
 - [34] E. Epelbaum, H. W. Hammer and U. G. Meissner, Modern Theory of Nuclear Forces, *Rev. Mod. Phys.* **81**, 1773 (2009).
 - [35] R. Machleidt and D. R. Entem, Chiral effective field theory and nuclear forces, *Phys. Rept.* **503**, 1 (2011).
 - [36] U. G. Meissner, *Phys. Scripta* **91**, no. 3, 033005 (2016).
 - [37] H. X. Chen, W. Chen, X. Liu and S. L. Zhu, The hidden-charm pentaquark and tetraquark states, *Phys. Rept.* **639**, 1 (2016).
 - [38] S. K. Choi *et al.* [Belle Collaboration], Observation of a narrow charmonium-like state in exclusive $B^{+(-)} \rightarrow K^{+(-)} \pi^+ \pi^- J/\psi$ decays, *Phys. Rev. Lett.* **91**, 262001 (2003).
 - [39] S. Godfrey and N. Isgur, Mesons in a Relativized Quark Model with Chromodynamics, *Phys. Rev. D* **32**, 189 (1985).
 - [40] R. Aaij *et al.* [LHCb Collaboration], Observation of $J/\psi p$ Resonances Consistent with Pentaquark States in $\Lambda_b^0 \rightarrow J/\psi K^- p$ Decays, *Phys. Rev. Lett.* **115**, 072001 (2015).
 - [41] V. M. Abazov *et al.* [D0 Collaboration], Evidence for a $B_s^0 \pi^\pm$ state, *Phys. Rev. Lett.* **117**, no. 2, 022003 (2016).
 - [42] R. Molina and E. Oset, The $Y(3940)$, $Z(3930)$ and the $X(4160)$ as dynamically generated resonances from the vector-vector interaction, *Phys. Rev. D* **80**, 114013 (2009).
 - [43] F. Aceti, M. Bayar, E. Oset, A. Martinez Torres, K. P. Khemchandani, J. M. Dias, F. S. Navarra and M. Nielsen, Prediction of an $I = 1$ $D\bar{D}^*$ state and relationship to the claimed $Z_c(3900)$, $Z_c(3885)$, *Phys. Rev. D* **90**, no. 1, 016003 (2014).
 - [44] J. He, The $Z_c(3900)$ as a resonance from the $D\bar{D}^*$ interaction, *Phys. Rev. D* **92**, no. 3, 034004 (2015).
 - [45] Q. R. Gong, Z. H. Guo, C. Meng, G. Y. Tang, Y. F. Wang and H. Q. Zheng, $Z_c(3900)$ as a $D\bar{D}^*$ molecule from the pole counting rule, *Phys. Rev. D* **94**, no. 11, 114019 (2016). [[arXiv:1604.08836 \[hep-ph\]](#)].
 - [46] Y. C. Yang, Z. Y. Tan, J. Ping and H. S. Zong, Possible $D^{(*)}\bar{D}^{(*)}$ and $B^{(*)}\bar{B}^{(*)}$ molecular states in the extended constituent quark models, [arXiv:1703.09718 \[hep-ph\]](#).
 - [47] M. T. AlFiky, F. Gabbiani and A. A. Petrov, $X(3872)$: Hadronic molecules in effective field theory, *Phys. Lett. B* **640**, 238 (2006).
 - [48] S. Fleming, M. Kusunoki, T. Mehen and U. van Kolck, Pion interactions in the $X(3872)$, *Phys. Rev. D* **76**, 034006 (2007).
 - [49] S. Fleming and T. Mehen, Hadronic Decays of the $X(3872)$ to $\chi(cJ)$ in Effective Field Theory, *Phys. Rev. D* **78**, 094019 (2008).
 - [50] V. Baru, A. A. Filin, C. Hanhart, Y. S. Kalashnikova, A. E. Kudryavtsev and A. V. Nefediev, Three-body $D\bar{D}\pi$ dynamics for the $X(3872)$, *Phys. Rev. D* **84**, 074029 (2011).
 - [51] M. P. Valderrama, Power Counting and Perturbative One Pion Exchange in Heavy Meson Molecules, *Phys. Rev. D* **85**, 114037 (2012).

- [52] J. Nieves and M. P. Valderrama, The Heavy Quark Spin Symmetry Partners of the $X(3872)$, *Phys. Rev. D* **86**, 056004 (2012).
- [53] C. Meng, J. J. Sanz-Cillero, M. Shi, D. L. Yao and H. Q. Zheng, Refined analysis on the $X(3872)$ resonance, *Phys. Rev. D* **92**, no. 3, 034020 (2015).
- [54] V. Baru, E. Epelbaum, A. A. Filin, J. Gegelia and A. V. Nefediev, Binding energy of the $X(3872)$ at unphysical pion masses, *Phys. Rev. D* **91**, no. 11, 114016 (2015).
- [55] V. Baru, E. Epelbaum, A. A. Filin, F.-K. Guo, H.-W. Hammer, C. Hanhart, U.-G. Meiner and A. V. Nefediev, Remarks on study of $X(3872)$ from effective field theory with pion-exchange interaction, *Phys. Rev. D* **91**, no. 3, 034002 (2015).
- [56] M. Jansen, H.-W. Hammer and Y. Jia, Finite volume corrections to the binding energy of the $X(3872)$, *Phys. Rev. D* **92**, no. 11, 114031 (2015).
- [57] E. Braaten, Galilean-invariant effective field theory for the $X(3872)$, *Phys. Rev. D* **91**, no. 11, 114007 (2015).
- [58] V. Baru, E. Epelbaum, A. A. Filin, C. Hanhart, U. G. Meissner and A. V. Nefediev, Heavy-quark spin symmetry partners of the $X(3872)$ revisited, *Phys. Lett. B* **763**, 20 (2016).
- [59] F. K. Guo, C. Hanhart, U. G. Meiner, Q. Wang, Q. Zhao and B. S. Zou, Hadronic molecules, [arXiv:1705.00141 \[hep-ph\]](#).
- [60] Y. R. Liu, X. Liu, W. Z. Deng and S. L. Zhu, Is $X(3872)$ Really a Molecular State?, *Eur. Phys. J. C* **56**, 63 (2008).
- [61] X. Liu, Z. G. Luo, Y. R. Liu and S. L. Zhu, $X(3872)$ and Other Possible Heavy Molecular States, *Eur. Phys. J. C* **61**, 411 (2009).
- [62] I. W. Lee, A. Faessler, T. Gutsche and V. E. Lyubovitskij, $X(3872)$ as a molecular DD^* state in a potential model, *Phys. Rev. D* **80**, 094005 (2009).
- [63] N. Li and S. L. Zhu, Isospin breaking, Coupled-channel effects and Diagnosis of $X(3872)$, *Phys. Rev. D* **86**, 074022 (2012).
- [64] E. Epelbaum, U. G. Meissner, W. Gloeckle and C. Elster, Resonance saturation for four nucleon operators, *Phys. Rev. C* **65**, 044001 (2002).
- [65] M. Mattson *et al.* [SELEX Collaboration], First observation of the doubly charmed baryon Ξ_{cc}^+ , *Phys. Rev. Lett.* **89**, 112001 (2002).
- [66] B. Aubert *et al.* [BaBar Collaboration], Search for doubly charmed baryons Ξ_{cc}^+ and Ξ_{cc}^{++} in BABAR, *Phys. Rev. D* **74**, 011103 (2006).
- [67] R. Aaij *et al.* [LHCb Collaboration], Search for the doubly charmed baryon Ξ_{cc}^+ , *JHEP* **1312**, 090 (2013).
- [68] R. Aaij *et al.* [LHCb Collaboration], Observation of the doubly charmed baryon Ξ_{cc}^{++} , [arXiv:1707.01621 \[hep-ex\]](#).
- [69] Z. F. Sun, Z. W. Liu, X. Liu and S. L. Zhu, Masses and axial currents of the doubly charmed baryons, *Phys. Rev. D* **91**, no. 9, 094030 (2015).
- [70] J. Hu and T. Mehen, Chiral Lagrangian with heavy quark-diquark symmetry, *Phys. Rev. D* **73**, 054003 (2006).
- [71] F. S. Yu, H. Y. Jiang, R. H. Li, C. D. L. W. Wang and Z. X. Zhao, Discovery Potentials of Doubly Charmed Baryons, [arXiv:1703.09086 \[hep-ph\]](#).
- [72] H. X. Chen, W. Chen, X. Liu, Y. R. Liu and S. L. Zhu, A review of the open charm and open bottom systems, *Rept. Prog. Phys.* **80**, no. 7, 076201 (2017).
- [73] H. X. Chen, Q. Mao, W. Chen, X. Liu and S. L. Zhu, Establishing low-lying doubly charmed baryons, [arXiv:1707.01779 \[hep-ph\]](#).
- [74] H. S. Li, L. Meng, Z. W. Liu and S. L. Zhu, Magnetic moments of the doubly charmed and bottomed baryons, [arXiv:1707.02765 \[hep-ph\]](#).
- [75] W. Wang, Z. P. Xing and J. Xu, Weak Decays of Doubly Heavy Baryons: SU(3) Analysis, [arXiv:1707.06570 \[hep-ph\]](#).
- [76] M. Karliner and J. L. Rosner, Quark-level analogue of nuclear fusion with doubly-heavy baryons, [arXiv:1708.02547 \[hep-ph\]](#).
- [77] S. Ohkoda, Y. Yamaguchi, S. Yasui, K. Sudoh and A. Hosaka, Exotic mesons with double charm and bottom flavor, *Phys. Rev. D* **86**, 034019 (2012).
- [78] N. Li, Z. F. Sun, X. Liu and S. L. Zhu, Coupled-channel analysis of the possible $D^{(*)}D^{(*)}$, $\bar{B}^{(*)}\bar{B}^{(*)}$ and $D^{(*)}\bar{B}^{(*)}$ molecular states, *Phys. Rev. D* **88**, 114008 (2013).
- [79] L. M. Abreu, Hadronic states with both open charm and bottom in effective field theory, *Nucl. Phys. A* **940**, 1 (2015).
- [80] S. Sakai, L. Roca and E. Oset, Charm-beauty meson bound states from $B(B^*)D(D^*)$ and $B(B^*)\bar{D}(\bar{D}^*)$ interaction, [arXiv:1704.02196 \[hep-ph\]](#).
- [81] W. Detmold, K. Orginos and M. J. Savage, BB Potentials in Quenched Lattice QCD, *Phys. Rev. D* **76**, 114503 (2007).
- [82] P. Bicudo, K. Cichy, A. Peters and M. Wagner, BB interactions with static bottom quarks from Lattice QCD, *Phys. Rev. D* **93**, no. 3, 034501 (2016).
- [83] A. Francis, R. J. Hudspith, R. Lewis and K. Maltman, Lattice Prediction for Deeply Bound Doubly Heavy Tetraquarks, *Phys. Rev. Lett.* **118**, no. 14, 142001 (2017).
- [84] Z. W. Liu, N. Li and S. L. Zhu, Chiral perturbation theory and the $\bar{B}\bar{B}$ strong interaction, *Phys. Rev. D* **89**, 074015 (2014).
- [85] G. Burdman and J. F. Donoghue, Union of chiral and heavy quark symmetries, *Phys. Lett. B* **280**, 287 (1992).
- [86] M. B. Wise, Chiral perturbation theory for hadrons containing a heavy quark, *Phys. Rev. D* **45**, no. 7, R2188 (1992).
- [87] T. M. Yan, H. Y. Cheng, C. Y. Cheung, G. L. Lin, Y. C. Lin and H. L. Yu, Heavy quark symmetry and chiral dynamics, *Phys. Rev. D* **46**, 1148 (1992), Erratum: [*Phys. Rev. D* **55**, 5851 (1997)].
- [88] S. L. Zhu, C. M. Maekawa, B. R. Holstein, M. J. Ramsey-Musolf and U. van Kolck, Nuclear parity-violation in effective field theory, *Nucl. Phys. A* **748**, 435 (2005).
- [89] D. Gülmöz, U.-G. Meißner and J. A. Oller, A chiral covariant approach to $\rho\rho$ scattering, *Eur. Phys. J. C* **77** (2017) no.7, 460.
- [90] Z. F. Sun, J. He, X. Liu, Z. G. Luo and S. L. Zhu, $Z_b(10610)^+$ and $Z_b(10650)^+$ as the $B^*\bar{B}$ and $B^*\bar{B}^*$ molecular states, *Phys. Rev. D* **84**, 054002 (2011).
- [91] Z. F. Sun, Z. G. Luo, J. He, X. Liu and S. L. Zhu, A note on the $B^*\bar{B}$, $B^*\bar{B}^*$, $D^*\bar{D}$, $D^*\bar{D}^*$, molecular states, *Chin. Phys. C* **36**, 194 (2012).
- [92] A. Abada, D. Becirevic, P. Boucaud, G. Herdoiza, J. P. Leroy, A. Le Yaouanc, O. Pene and J. Rodriguez-Quintero, First lattice QCD estimate of the $g_{D^*\pi}$ coupling, *Phys. Rev. D* **66**, 074504 (2002).
- [93] D. Becirevic and F. Sanfilippo, Theoretical estimate of the $D^* \rightarrow D\pi$ decay rate, *Phys. Lett. B* **721**, 94 (2013).
- [94] K. U. Can, G. Erkol, M. Oka, A. Ozpineci and T. T. Takahashi, Vector and axial-vector couplings of D and D^* mesons in 2+1 flavor Lattice QCD, *Phys. Lett. B* **719**, 103 (2013).
- [95] P. Colangelo, G. Nardulli, A. Deandrea, N. Di Bartolomeo, R. Gatto and F. Feruglio, On the coupling of heavy mesons to pions in QCD, *Phys. Lett. B* **339**, 151 (1994).
- [96] V. M. Belyaev, V. M. Braun, A. Khodjamirian and R. Ruckl, $D^*D\pi$ and $B^*B\pi$ couplings in QCD, *Phys. Rev. D* **51**, 6177 (1995).
- [97] H. G. Dosch and S. Narison, $B^*B\pi$ couplings and $D^* \rightarrow D\pi$ decays within a $1/M$ expansion in full QCD, *Phys. Lett. B* **368**, 163 (1996).
- [98] P. Colangelo and F. De Fazio, QCD interactions of heavy mesons with pions by light cone sum rules,

- [Eur. Phys. J. C **4**, 503 \(1998\).](#)
- [99] M. E. Bracco, M. Chiapparini, F. S. Navarra and M. Nielsen, Charm couplings and form factors in QCD sum rules, [Prog. Part. Nucl. Phys. **67**, 1019 \(2012\).](#)
- [100] P. Colangelo, F. De Fazio and G. Nardulli, D^* radiative decays and strong coupling of heavy mesons with soft pions in a QCD relativistic potential model, [Phys. Lett. B **334**, 175 \(1994\).](#)
- [101] D. Becirevic and A. Le Yaouanc, G coupling ($g_{B^*B\pi}$, $g_{D^*D\pi}$): A Quark model with Dirac equation, [JHEP **9903**, 021 \(1999\).](#)
- [102] B. El-Bennich, M. A. Ivanov and C. D. Roberts, Strong $D^* \rightarrow D\pi$ and $B^* \rightarrow B\pi$ couplings, [Phys. Rev. C **83**, 025205 \(2011\).](#)
- [103] C. Patrignani *et al.* [Particle Data Group], Review of Particle Physics, [Chin. Phys. C **40**, no. 10, 100001 \(2016\).](#)
- [104] G. Ecker, J. Gasser, A. Pich and E. de Rafael, The Role of Resonances in Chiral Perturbation Theory, [Nucl. Phys. B **321**, 311 \(1989\).](#)
- [105] J. F. Donoghue, C. Ramirez and G. Valencia, The Spectrum of QCD and Chiral Lagrangians of the Strong and Weak Interactions, [Phys. Rev. D **39**, 1947 \(1989\).](#)
- [106] V. Bernard, N. Kaiser and U. G. Meissner, Aspects of chiral pion - nucleon physics, [Nucl. Phys. A **615**, 483 \(1997\).](#)
- [107] M. L. Du, F. K. Guo, U. G. Meissner and D. L. Yao, Aspects of the low-energy constants in the chiral Lagrangian for charmed mesons, [Phys. Rev. D **94**, no. 9, 094037 \(2016\).](#)
- [108] J. X. Lu, L. S. Geng and M. P. Valderrama, Heavy Baryon Molecules in Effective Field Theory, [arXiv:1706.02588 \[hep-ph\].](#)
- [109] D. B. Kaplan, M. J. Savage and M. B. Wise, A New expansion for nucleon-nucleon interactions, [Phys. Lett. B **424**, 390 \(1998\).](#)
- [110] J. Nieves, Renormalization of the one pion exchange NN interaction in presence of derivative contact interactions, [Phys. Lett. B **568**, 109 \(2003\).](#)
- [111] J. F. Yang and J. H. Huang, Renormalization of NN scattering: Contact potential, [Phys. Rev. C **71**, 034001 \(2005\).](#)
- [112] M. Pavon Valderrama and E. Ruiz Arriola, Renormalization of NN interaction with chiral two pion exchange potential. central phases and the deuteron, [Phys. Rev. C **74**, 054001 \(2006\).](#)
- [113] M. Pavon Valderrama and E. Ruiz Arriola, Renormalization of NN interaction with chiral two pion exchange potential: Non-central phases, [Phys. Rev. C **74**, 064004 \(2006\)](#), Erratum: [Phys. Rev. C **75**, 059905 \(2007\).](#)
- [114] M. P. Valderrama, Power Counting and Wilsonian Renormalization in Nuclear Effective Field Theory, [Int. J. Mod. Phys. E **25**, no. 05, 1641007 \(2016\).](#)
- [115] W. A. Bardeen, E. J. Eichten and C. T. Hill, Chiral multiplets of heavy - light mesons, [Phys. Rev. D **68**, 054024 \(2003\).](#)